

**Modelling  
of  
Microstructural Evolutions  
in  
Structural Materials**

**Yoshiyuki Saito**

**Department of Electronic and Photonic Systems**

**Waseda University**

# Contents

## 1. Introduction

Present State

Target

## 2. Computational Models based on Thermodynamics and Phase Transformation Theory

## 3. Computer Simulation(Topics)

grain growth, spinodal decomposition

## 4. Future plan

**3-D multiscale, Nanostructural materials**

# Problems

## Modelling of microstructural evolutions in structural steels

- **Synergetic effects**

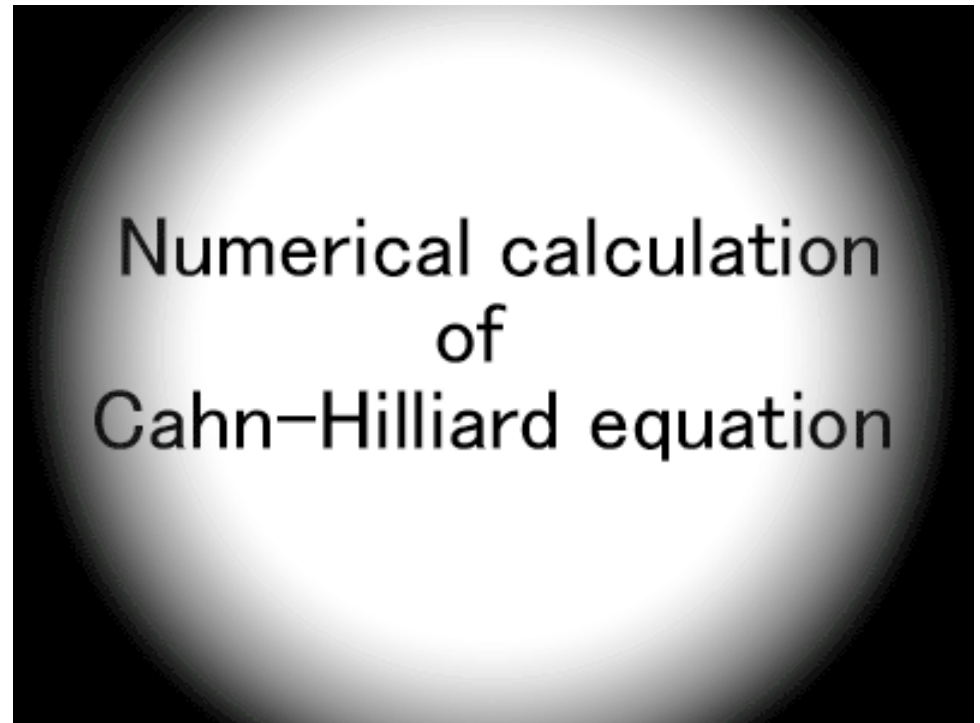
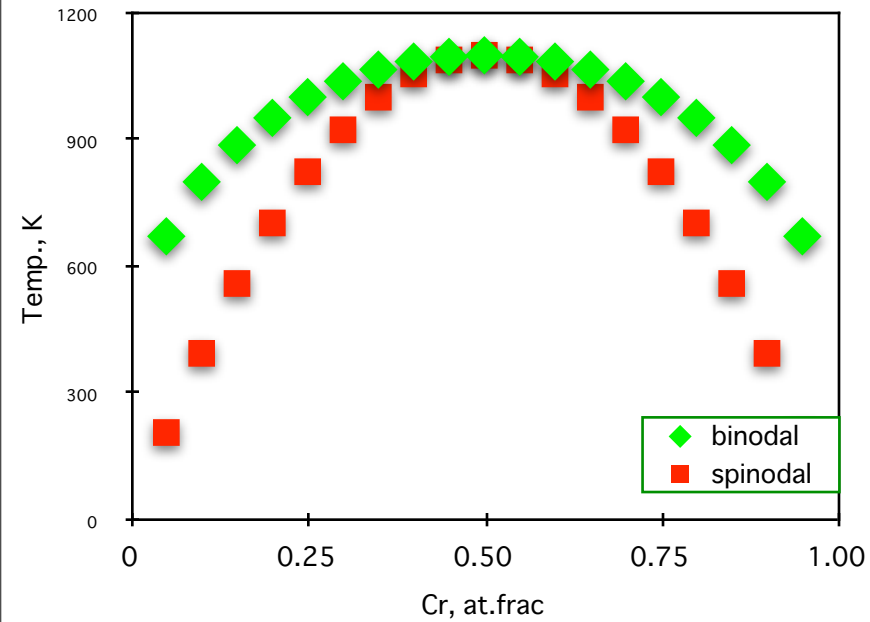
grain growth, recrystallization, second phase precipitation, spinodal decomposition,  $\gamma$  to  $\alpha$  phase transformation,

- **Multiscale**

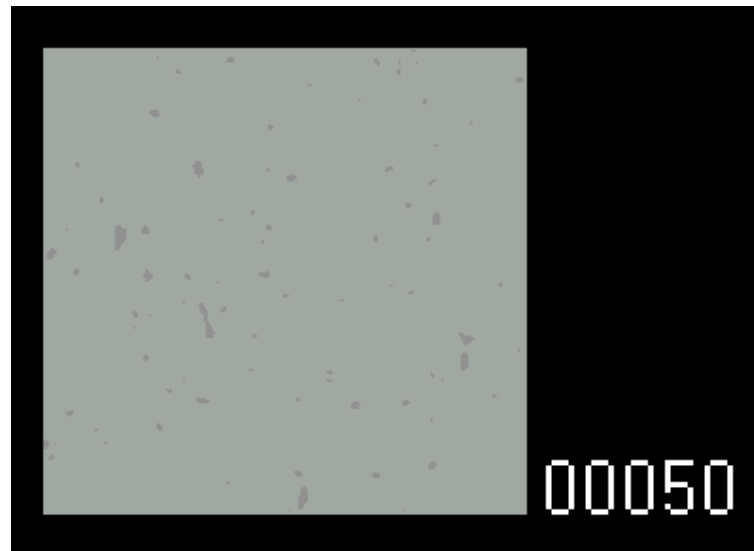
several nm to several hundred  $\mu$ m

- **Multicomponent system**

# Phase separation



# Grain growth



# Modelling of microstructural evolution in structural steel

- 1st stage(1985-1995)  
Integrated model based on thermodynamics and phase transformation theory
- 2nd stage(1995-2005)  
MC, PF for Grain growth, Spinodal decomposition etc.
- 3rd stage(2005- )  
Multiscale 3-D simulation for microstructural evolution in structural steel.

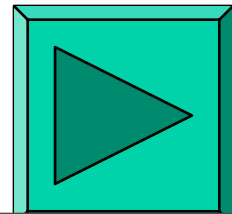
# **Computational Models based on Thermodynamics and Phase Transformation Theory**

## **1. Theories of Microstructural Evolution**

Nucleation, Growth and Interface Migration

## **2. Integrated Models for Predicting Microstructural Evolution in HSLA steels**

Grain growth, Precipitation, Phase Transformation



# Modelling of microstructural evolution in structural steel

- 1st stage(1985-1995)  
Integrated model based on thermodynamics and phase transformation theory
- 2nd stage(1995-2005)  
MC, PF for Grain growth, Spinodal decomposition etc.
- 3rd stage(2005- )  
Multiscale 3-D simulation for microstructural evolution in structural steel.



# Computer Simulation

- Discrete model

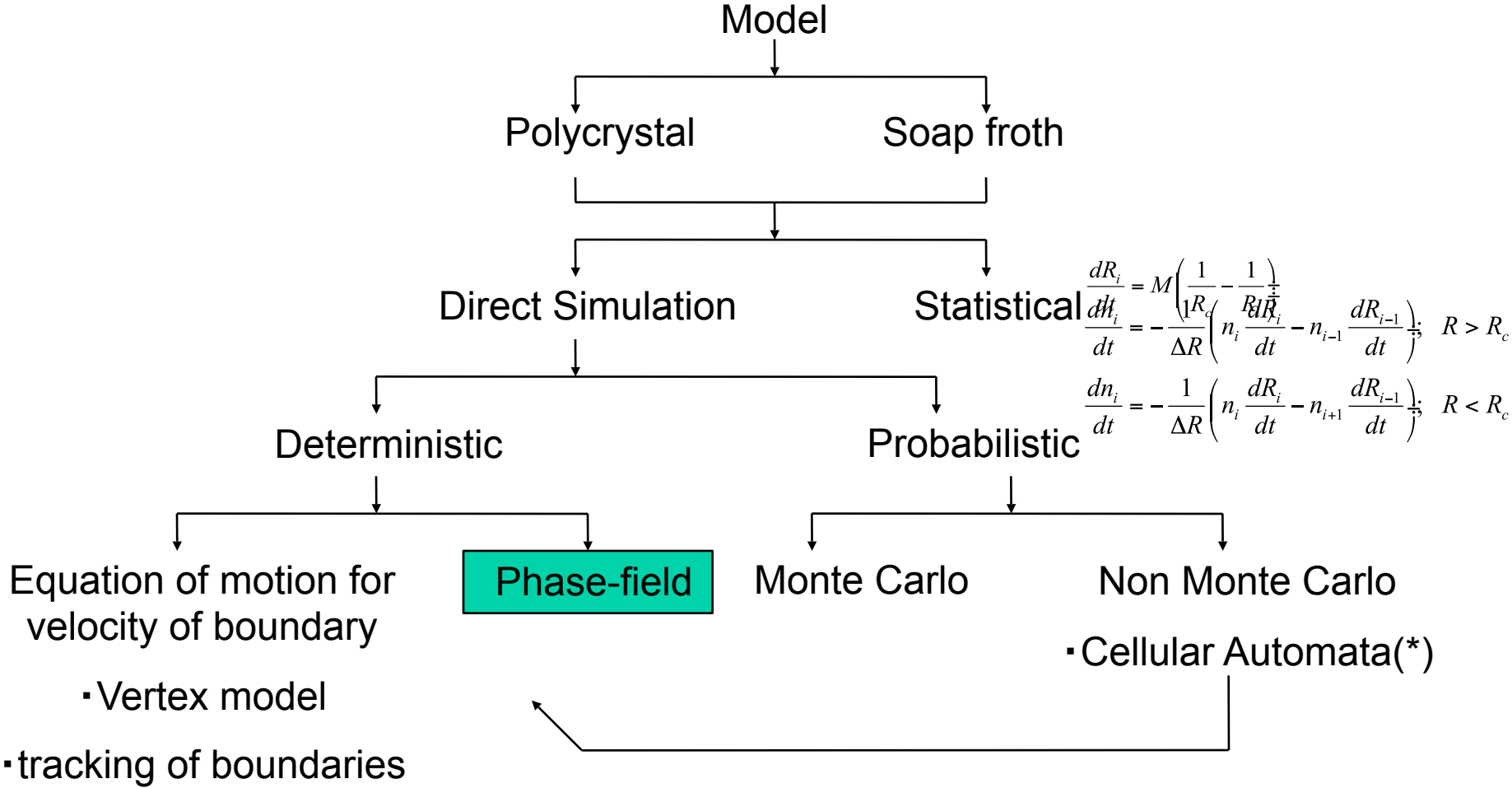
**Monte Carlo method**

- Continuum model

**Phase field model**

# Grain Growth

# Classification of simulation models



# Simulation of Grain Growth by

We can write the total free energy of an inhomogeneous system in terms of all the orientation field variables and their gradients as:

$$F = \int \left[ f_0(\eta_1, \eta_2, \dots, \eta_p) + \frac{1}{2} \sum_{i=1}^p k_i (\nabla \eta_i)^2 \right] dV$$

$f_0$  : the local free energy density

$k_i$  : the gradient energy coefficients

$p$  : total number of orientation field variable

Since the orientation field variables  $\eta_i$  are non-conserved order parameter, the temporal evolutions of these parameters are written as follows

$$\frac{\partial \eta_i(\vec{x}, t)}{\partial t} = -L_i \frac{\delta F}{\delta \eta_i(\vec{x}, t)}$$

$L_i$  : Onsager's phenomenological parameters (mobility of a interface)

# The Phase field model

Time dependent Ginzburg Landau (TDGL) equation

For conserved field variables

$$\frac{\partial \mathbf{c}(\mathbf{r}, t)}{\partial t} = M \nabla^2 \left( \frac{\delta F}{\delta \mathbf{c}(\mathbf{r}, t)} \right)$$

For nonconserved field variables

$$\frac{\partial \eta(\mathbf{r}, t)}{\partial t} = -L \left( \frac{\delta \tilde{F}}{\delta \eta(\mathbf{r}, t)} \right)$$

The free energy functional  $F$

$$\tilde{F} = \int \left[ F_{\text{chem}}(\mathbf{c}(\mathbf{r}, t), \eta(\mathbf{r}, t), T) + F_{\text{elas}}(\mathbf{c}(\mathbf{r}, t), \eta(\mathbf{r}, t), T) + F_{\text{int}}(\mathbf{c}(\mathbf{r}, t), \eta(\mathbf{r}, t), T) \right] d\mathbf{r}$$

# Simulation of grain growth

$\eta_1(\mathbf{r}), \eta_2(\mathbf{r}), \dots, \eta_p(\mathbf{r})$  ; a set of orientation field variables

The total free energy functional

$$F = \int \left[ f_0(\eta_1(\mathbf{r}), \eta_2(\mathbf{r}), \dots, \eta_p(\mathbf{r})) + \sum_{i=1}^p \frac{k_i}{2} (\nabla \eta_i(\mathbf{r}))^2 \right] d\mathbf{r}$$

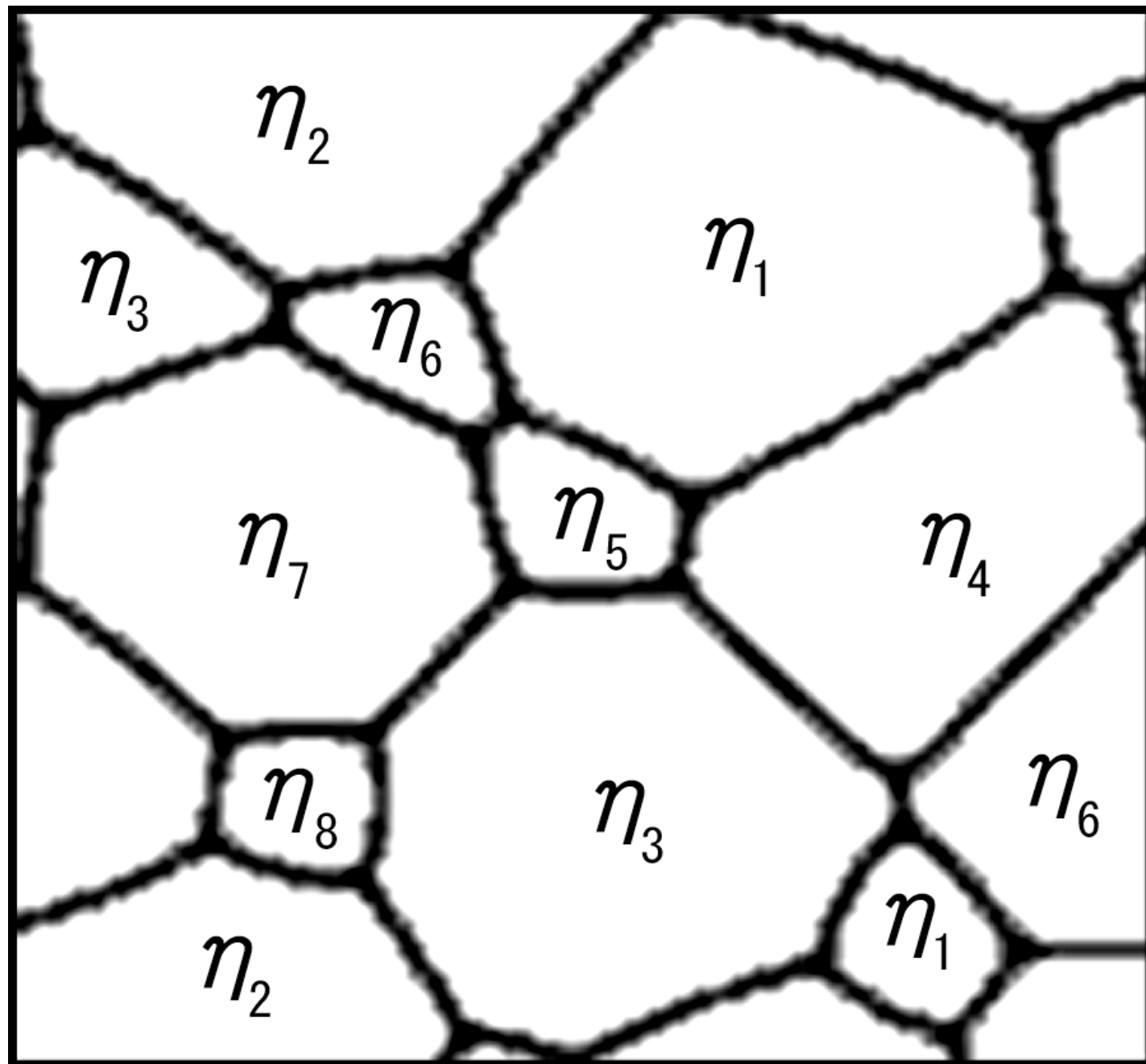
The spatial and temporal evolution of orientation field variables

$$\frac{\partial \eta_i(\mathbf{r}, t)}{\partial t} = -L_i \frac{\delta F}{\delta \eta_i(\mathbf{r}, t)} = -L_i \left( \frac{\partial f_0}{\partial \eta_i} - k_i \nabla^2 \eta_i \right) \quad i = 1, p$$

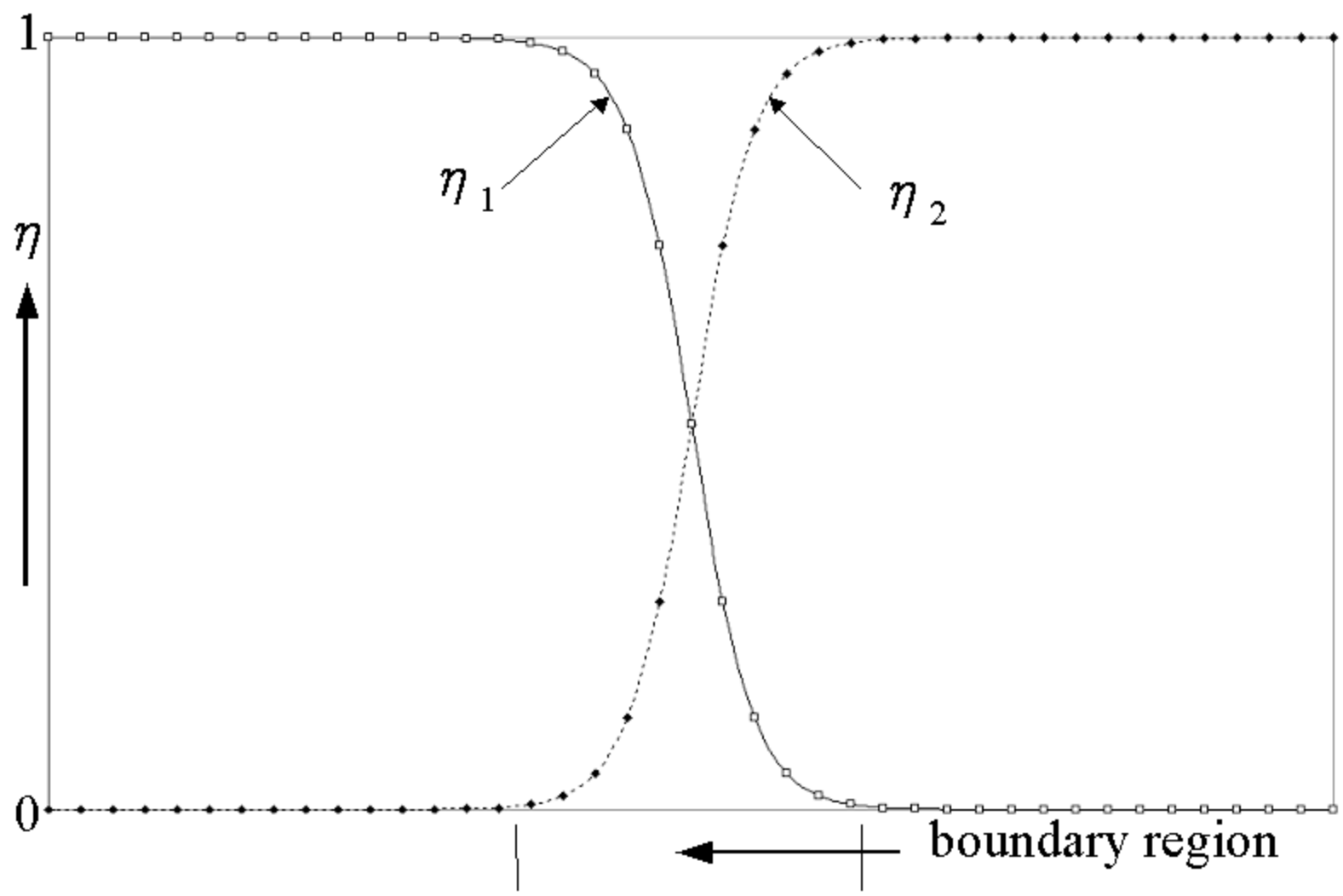
The Ginzburg-Landau type free energy density functional

$$f_0(\eta_1, \eta_2, \dots, \eta_p) = \sum_{i=1}^p \left( -\alpha \eta_i^2 / 2 + \beta \eta_i^4 \right) + \gamma \sum_{i=1}^p \sum_{j \neq i}^p \eta_i^2 \eta_j^2$$

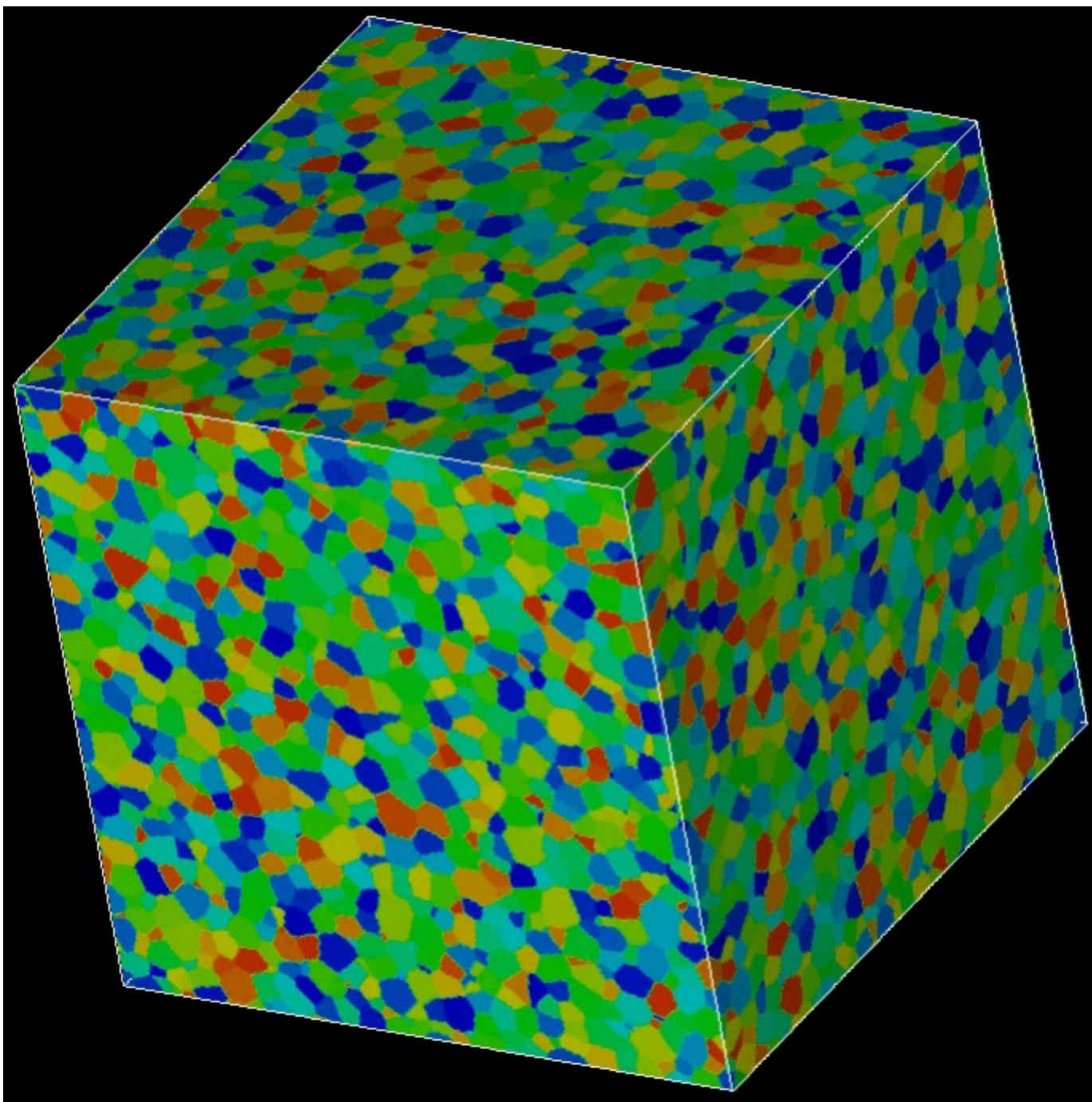
$\alpha, \beta, \gamma$  are phenomenological parameters.



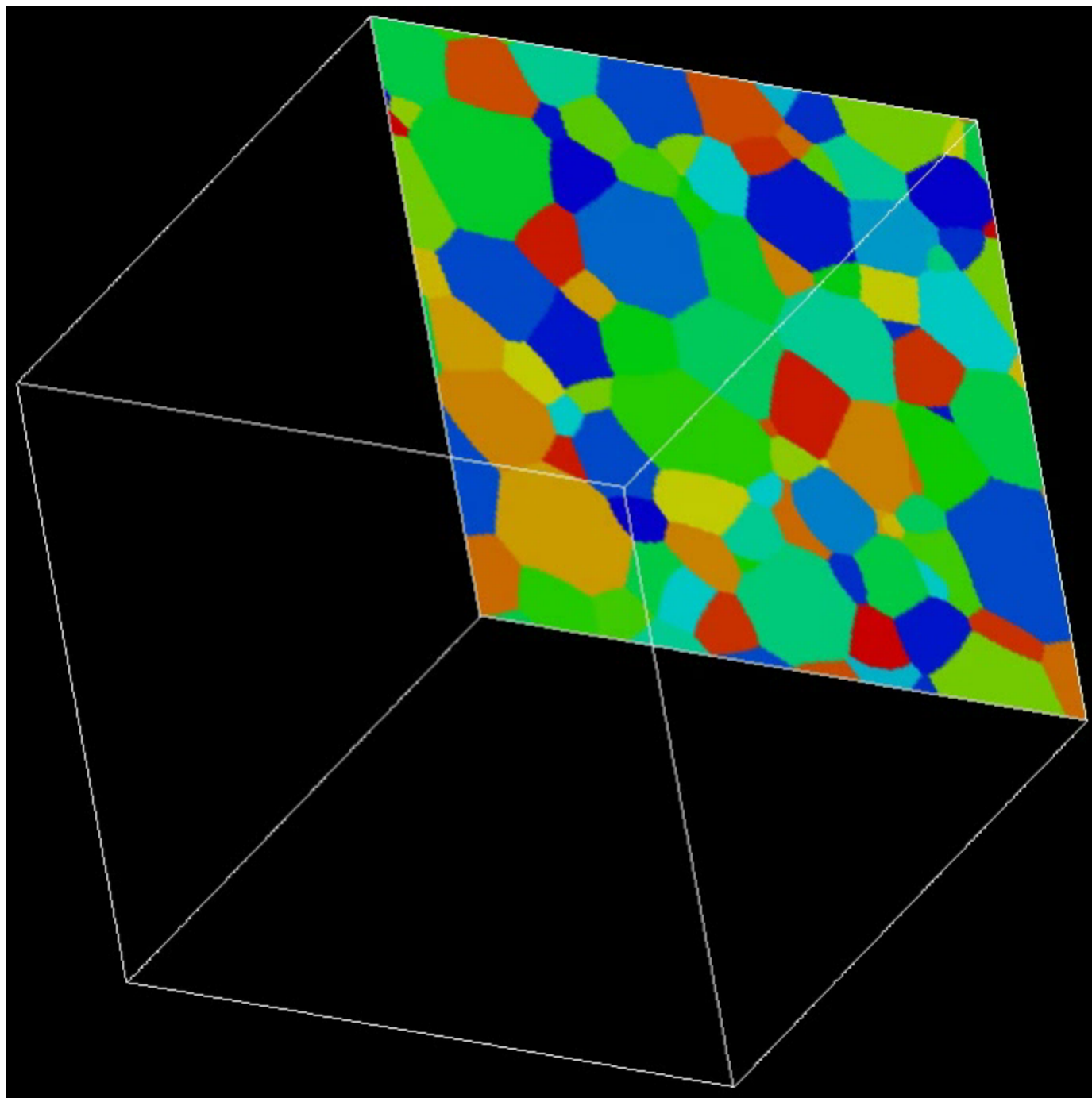


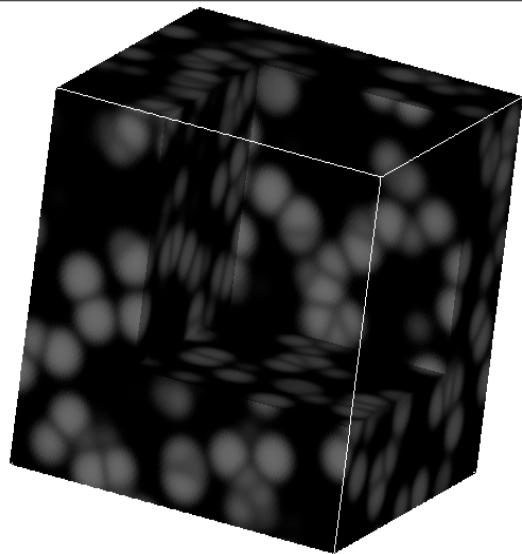




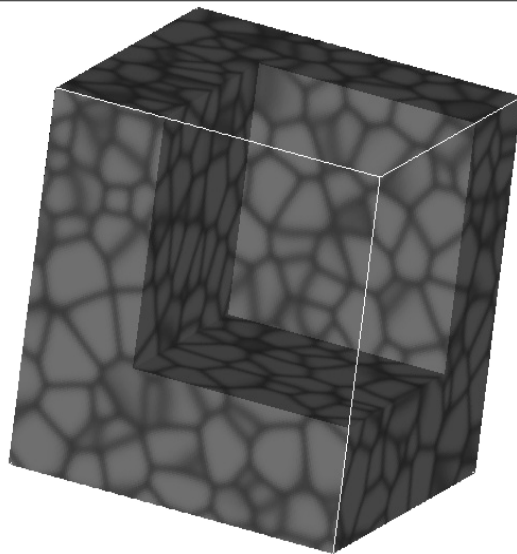




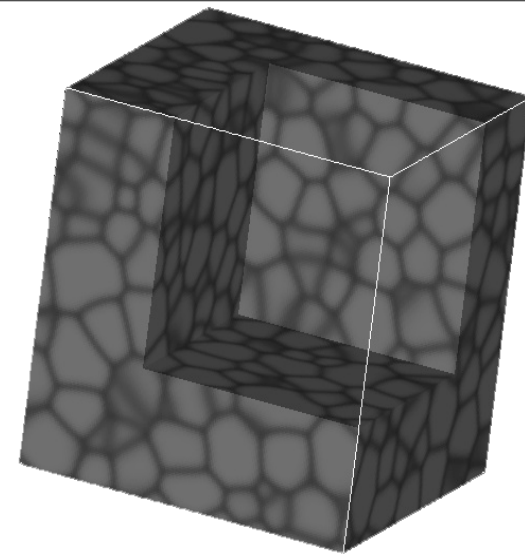




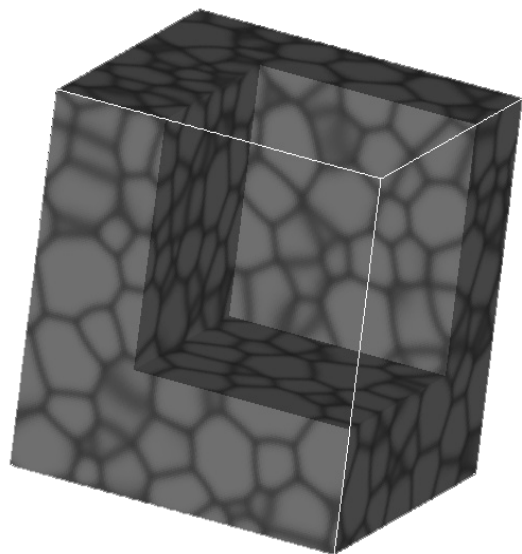
$t=10.0$



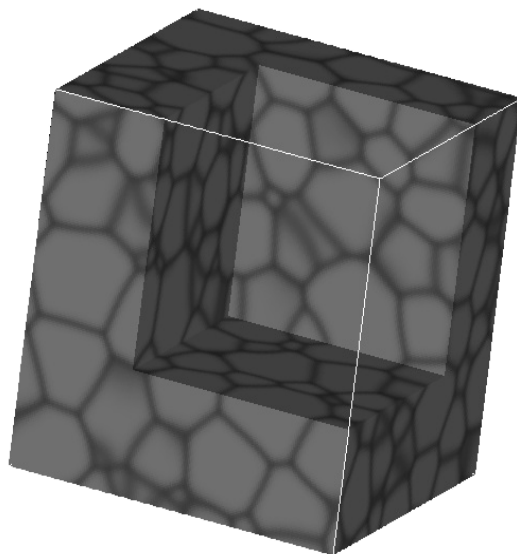
$t=20.0$



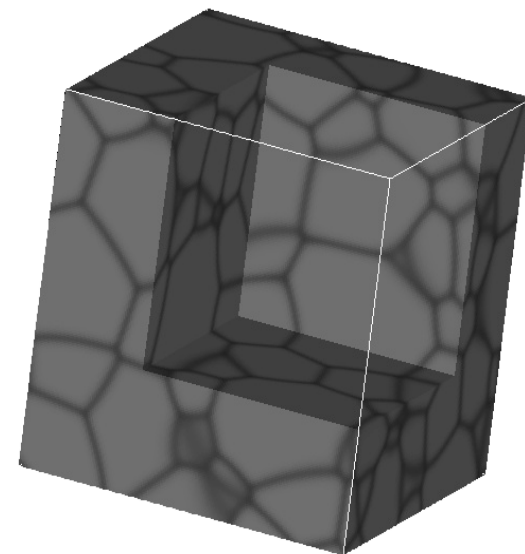
$t=50.0$



$t=100.0$



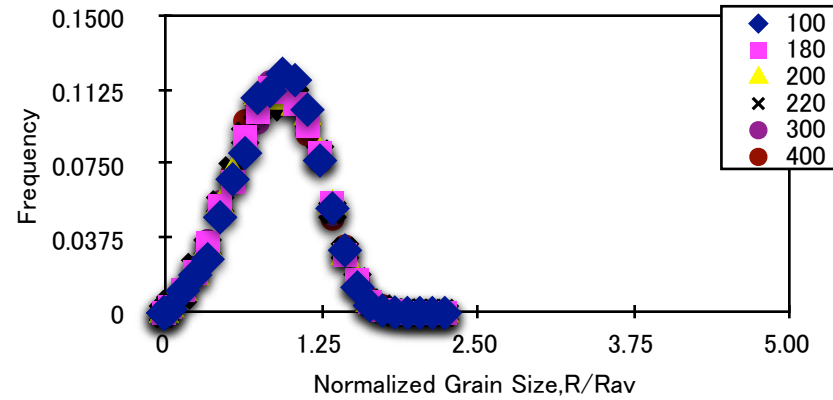
$t=200.0$



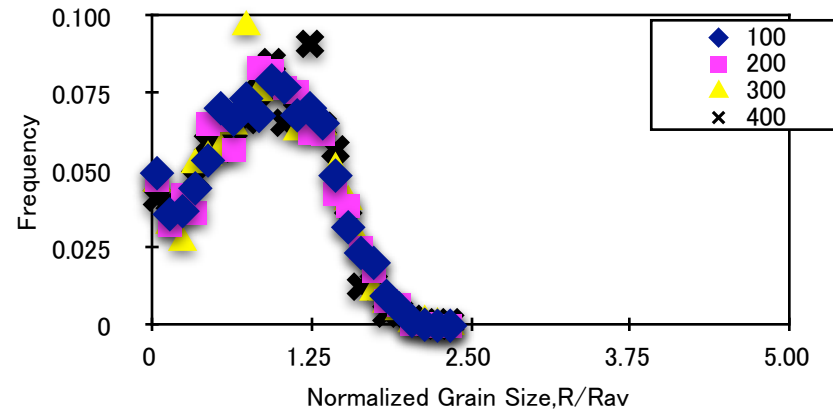
$t=500.0$

# -Isotropic Grain Growth

## •3D-simulation



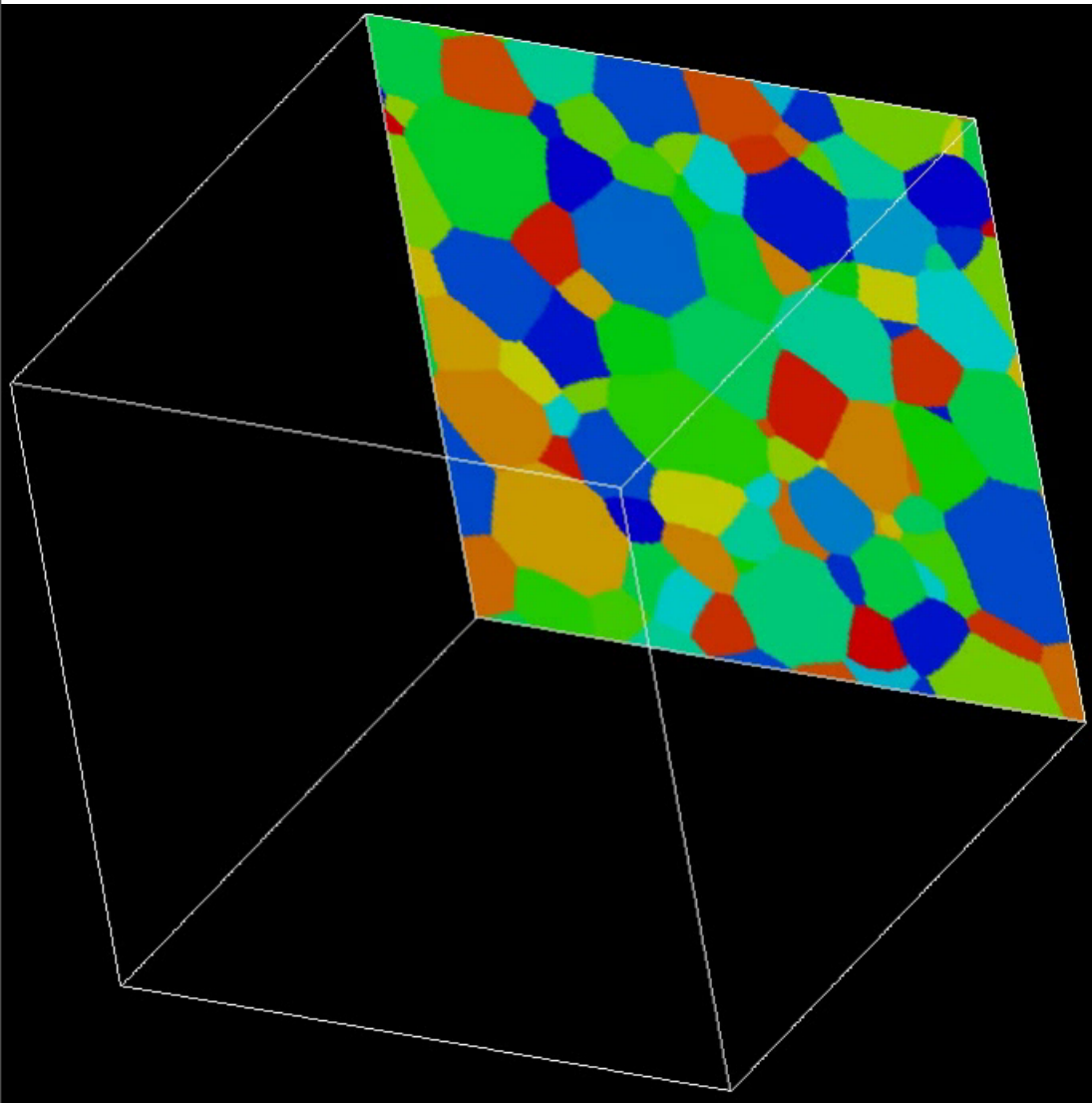
## •2D cross section of 3D simulation



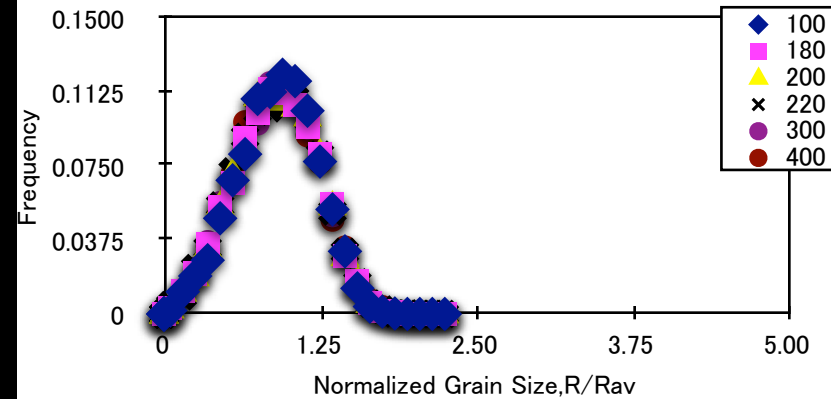
Variation in the scaled grain size distribution function

System size :  $320^3$

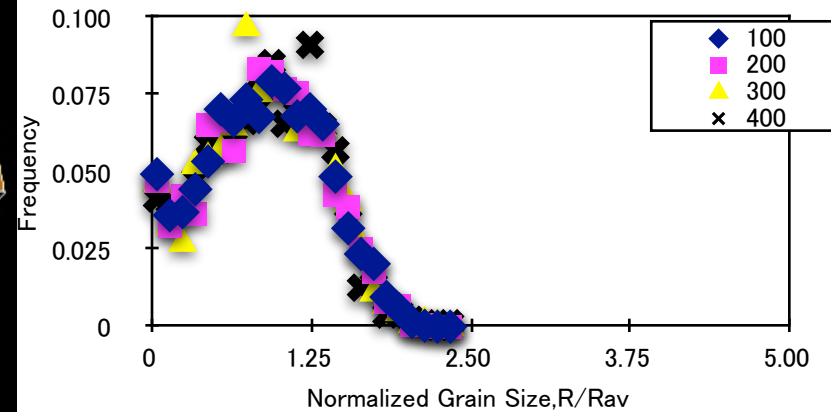
# -Isotropic Grain Growth



## •3D-simulation



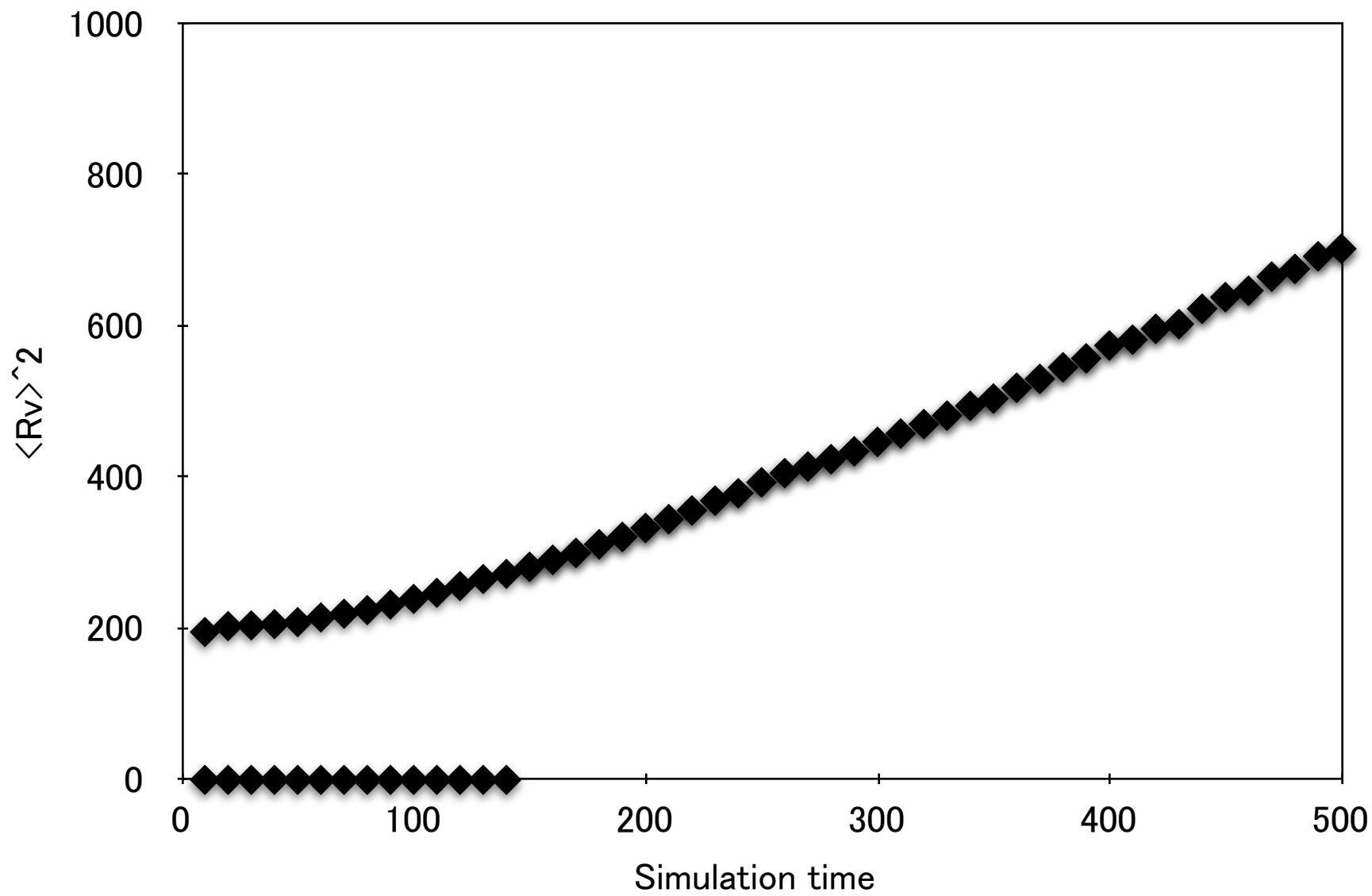
## •2D cross section of 3D simulation

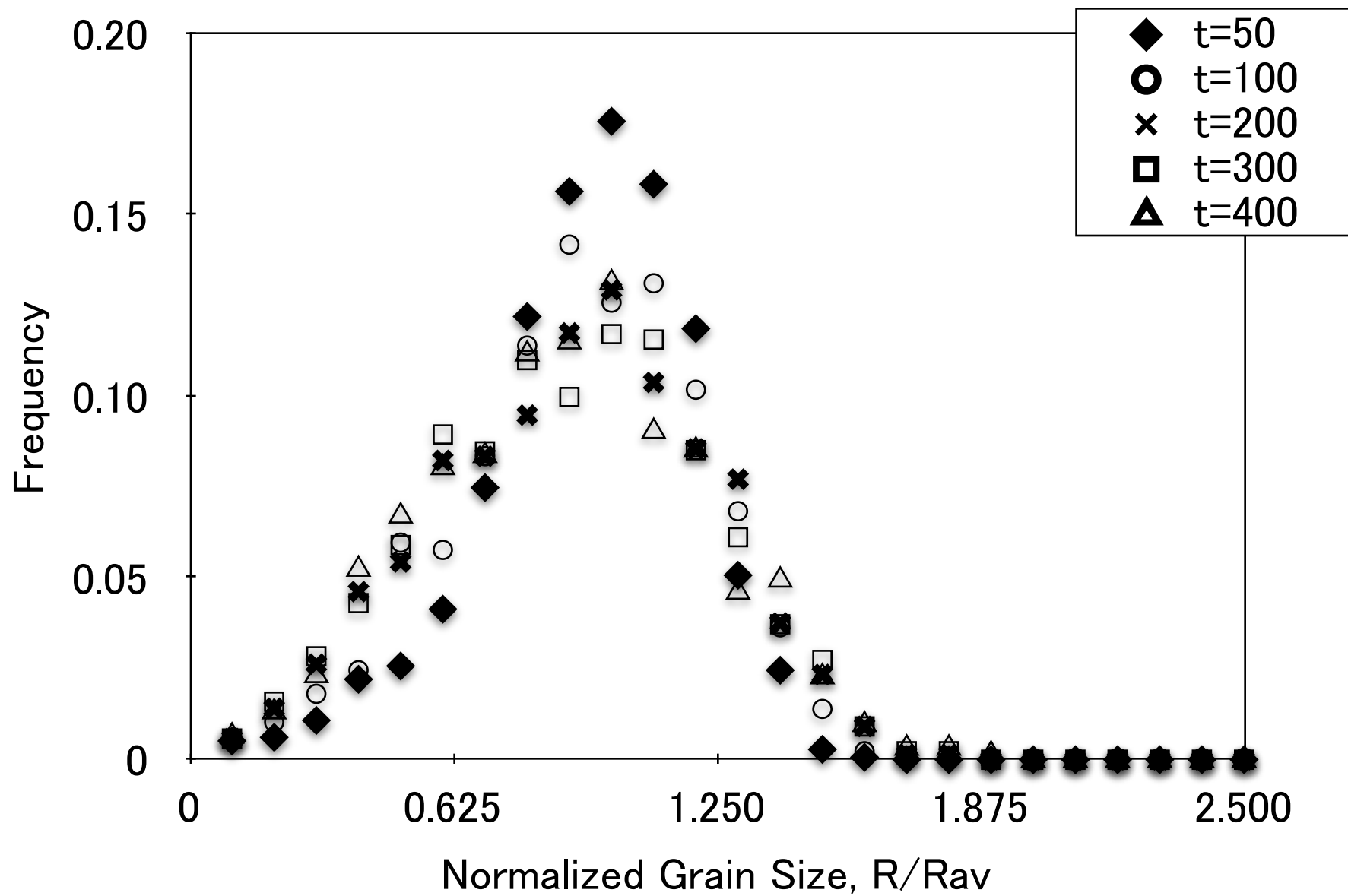


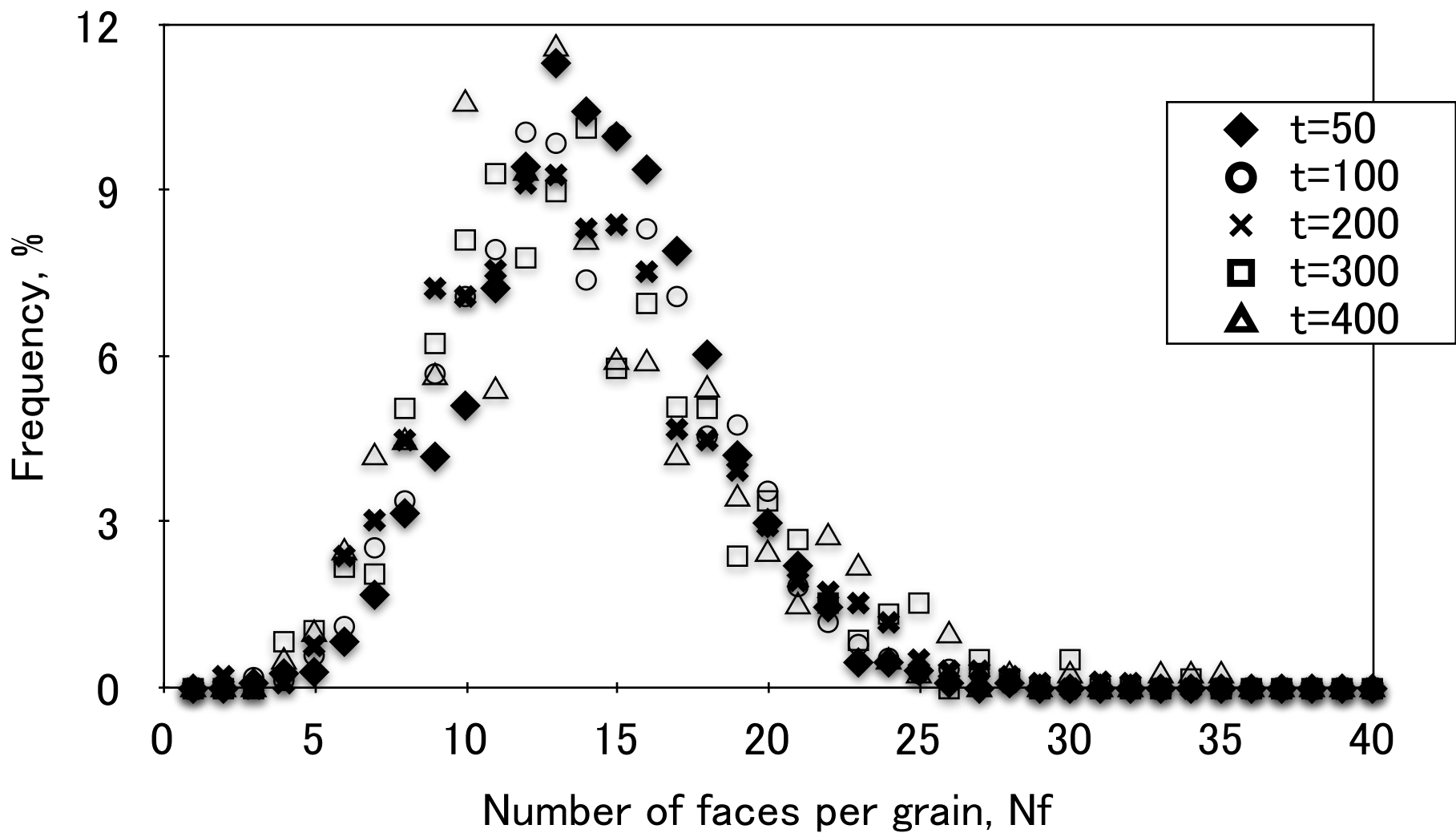
Variation in the scaled grain size distribution function

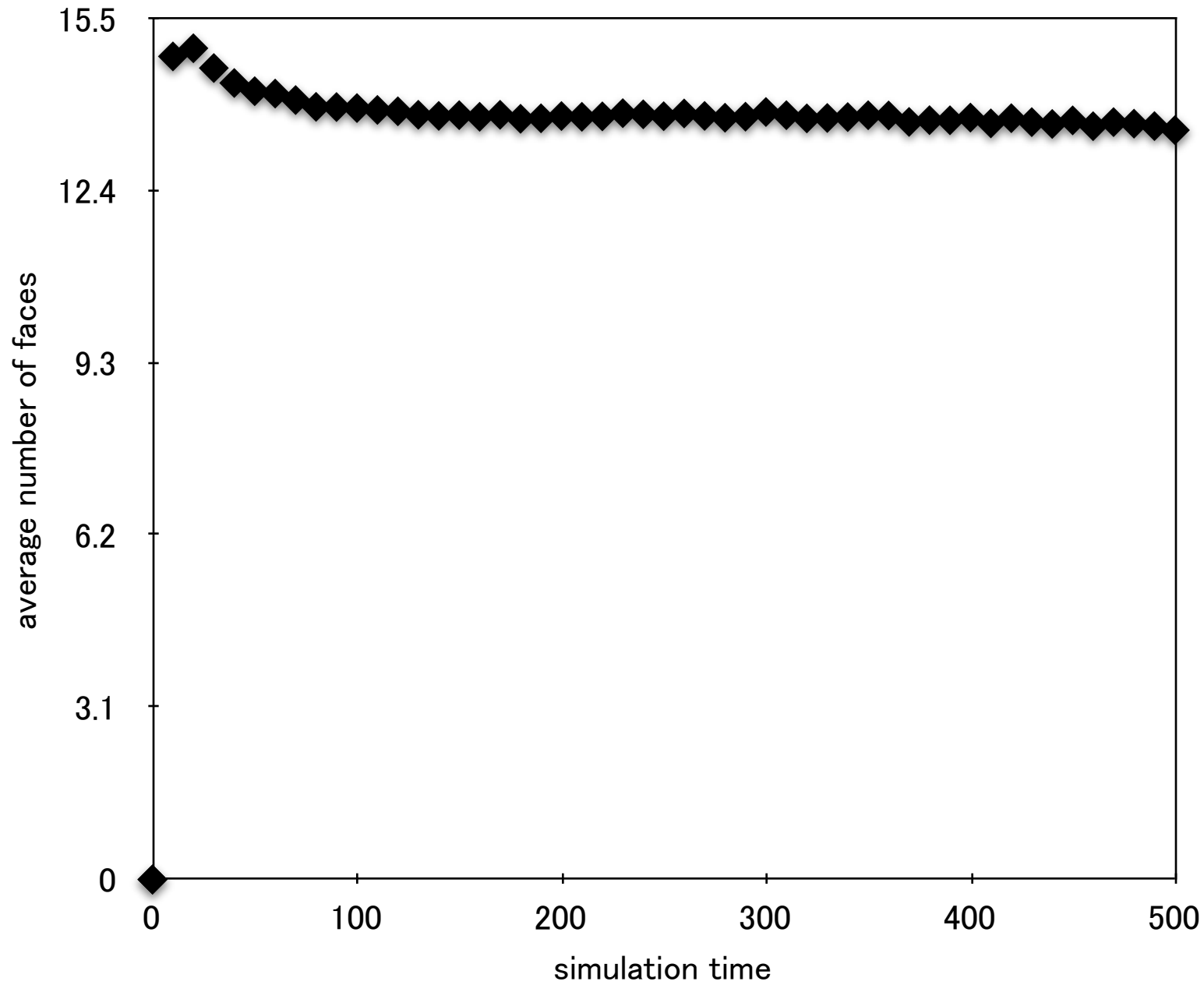
System size :  $320^3$

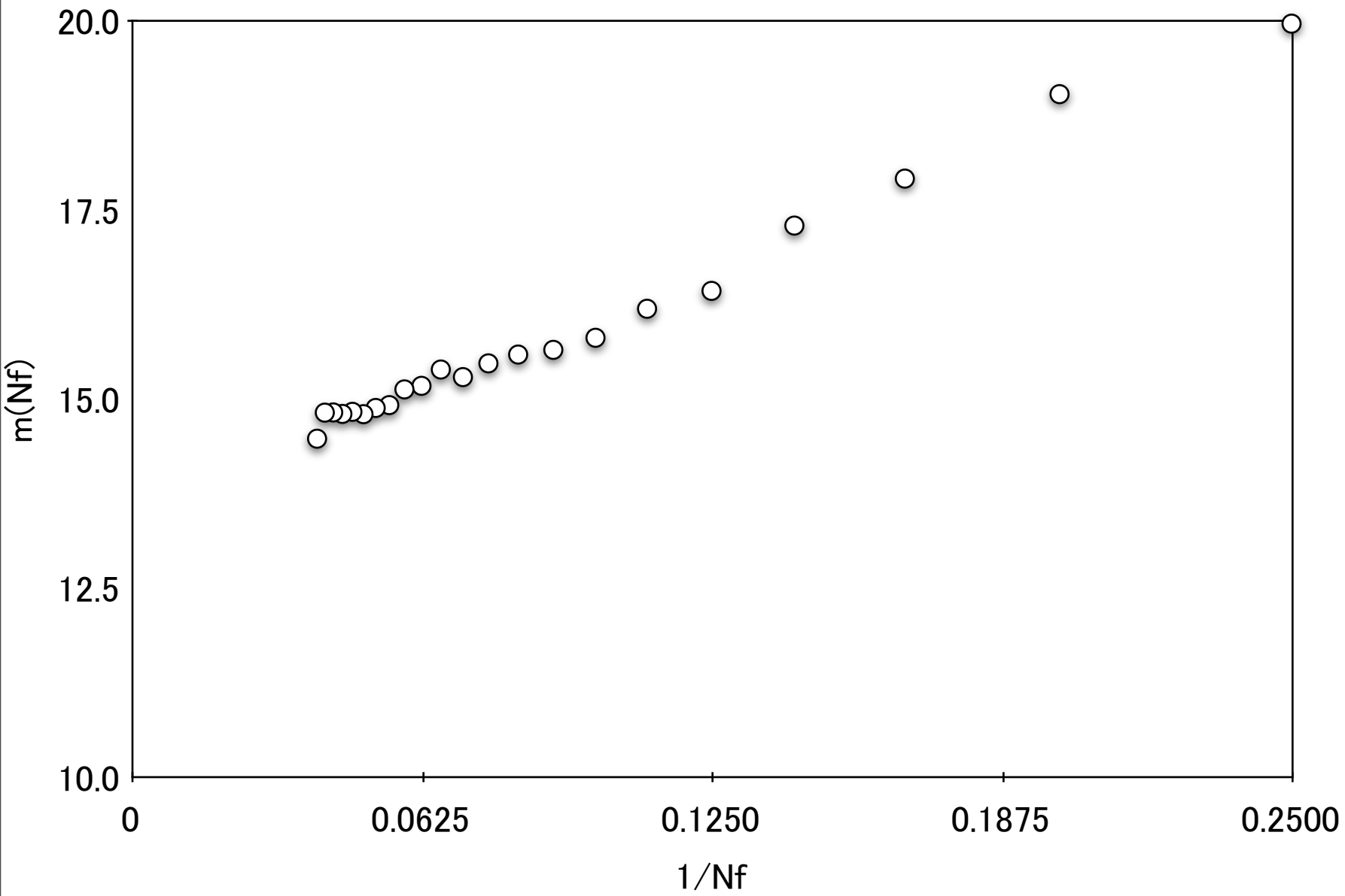












**Simulation of Grain Growth**  
**by**

# The Metropolis Algorithm

## Importance Sampling--- Markov process

A configuration  $\{s'\}$  is generated from the knowledge of a configuration  $\{s\}$ .

$W(\{s\},\{s'\})$ : the conditional probability to select  $\{s'\}$  starting from  $\{s\}$ .

The equilibrium distribution:

$$P_{\text{eq}}(\{s\}) = \exp[-E(\{s\})/k_B T] / Z.$$

$E$ : internal energy function,  $k_B$  : the Boltzmann constant,  
 $T$ : temperature ,  $Z$  : canonical partition function.

# The procedure of the simulation

- (1). A grain number from 1 to the system size,  $N$ , is assigned to each lattice point.
- (2). A number corresponds to an orientation is randomly assigned to each grain.
- (3). The evolution of microstructure is tracked by the change of orientations on each lattice
  - (a). One lattice site is selected at random .
  - (b). If the lattice site belongs to grain boundary, then a new orientation is generated.
  - (c). If one of nearest neighbor lattices has the same orientation as the newly selected grain orientation, a re-orientation trial is attempted.
  - (d). The change in energy,  $\Delta E$ , associated with the change of grain orientation is calculated. The re-orientation trial is accepted if  $\Delta E$  is less than or equal to zero. If the value  $\Delta E$  is greater than zero, the re-orientation is accepted with probability,

$$W = \exp(-\Delta E/k_B T).$$



# The change of interfacial energy accompanying re-orientation

- The interfacial energy is a function of the grain misorientation:

$$E_0 = - \sum_{\langle ij \rangle} M_{ij} s_i \cdot s_j,$$

$s_i$  ; grain orientation.

Matrix  $M_{ij}$

$$M_{ij} = J (1 - \delta_{ij})$$

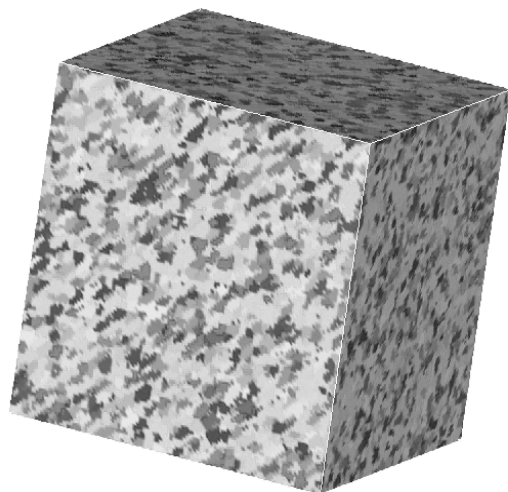
isotropic

$$M_{ij} = J (1 - \delta_{ij}) [1 - (1 - r) \delta_{i i+k}]$$

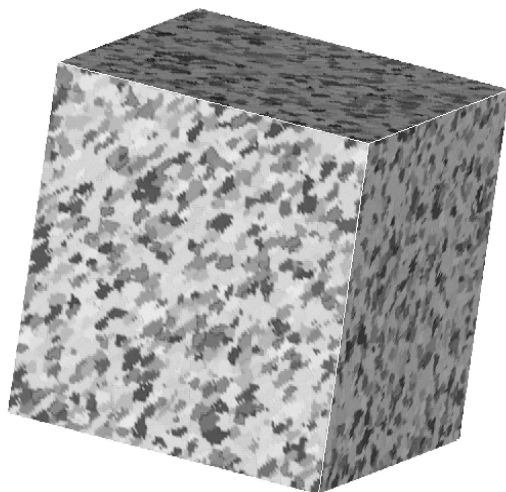
anisotropic

# Condition of the simulation

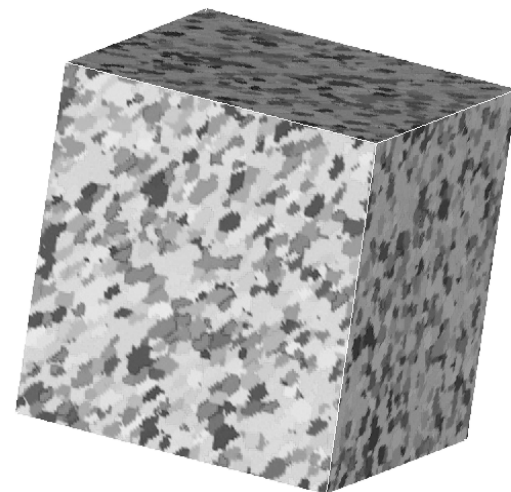
- System size:  $128^3$
- The number of orientation: 16 or 32
- 3-dimensional
- $J/K_B T = 0.75$



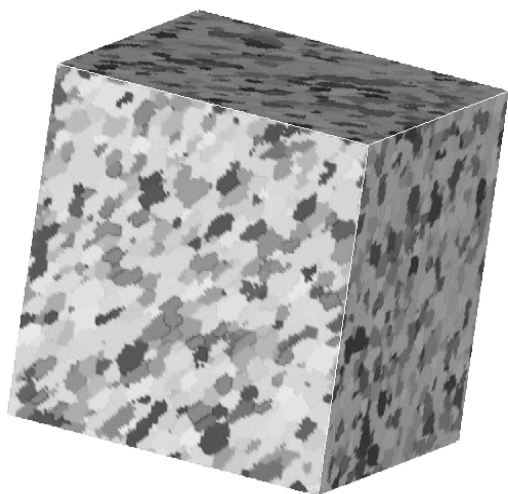
*100 MCS*



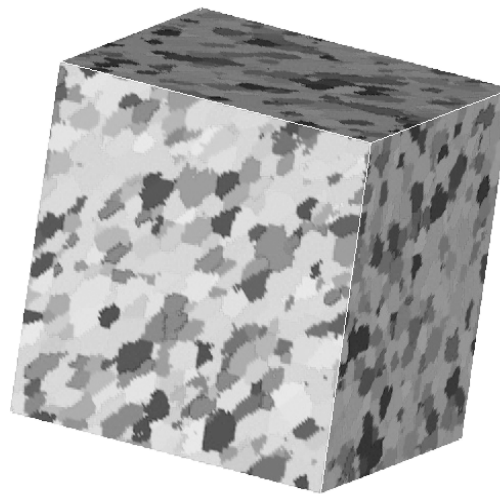
*200 MCS*



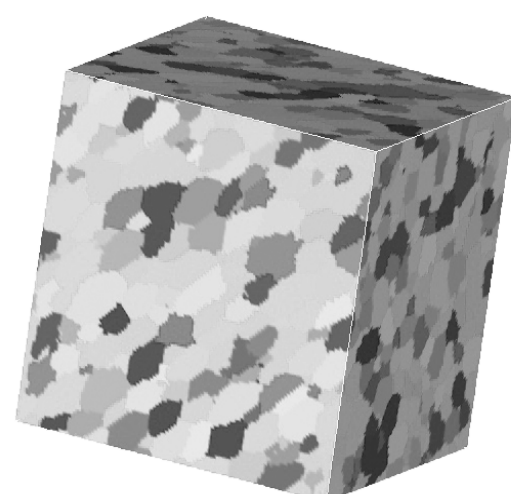
*500 MCS*



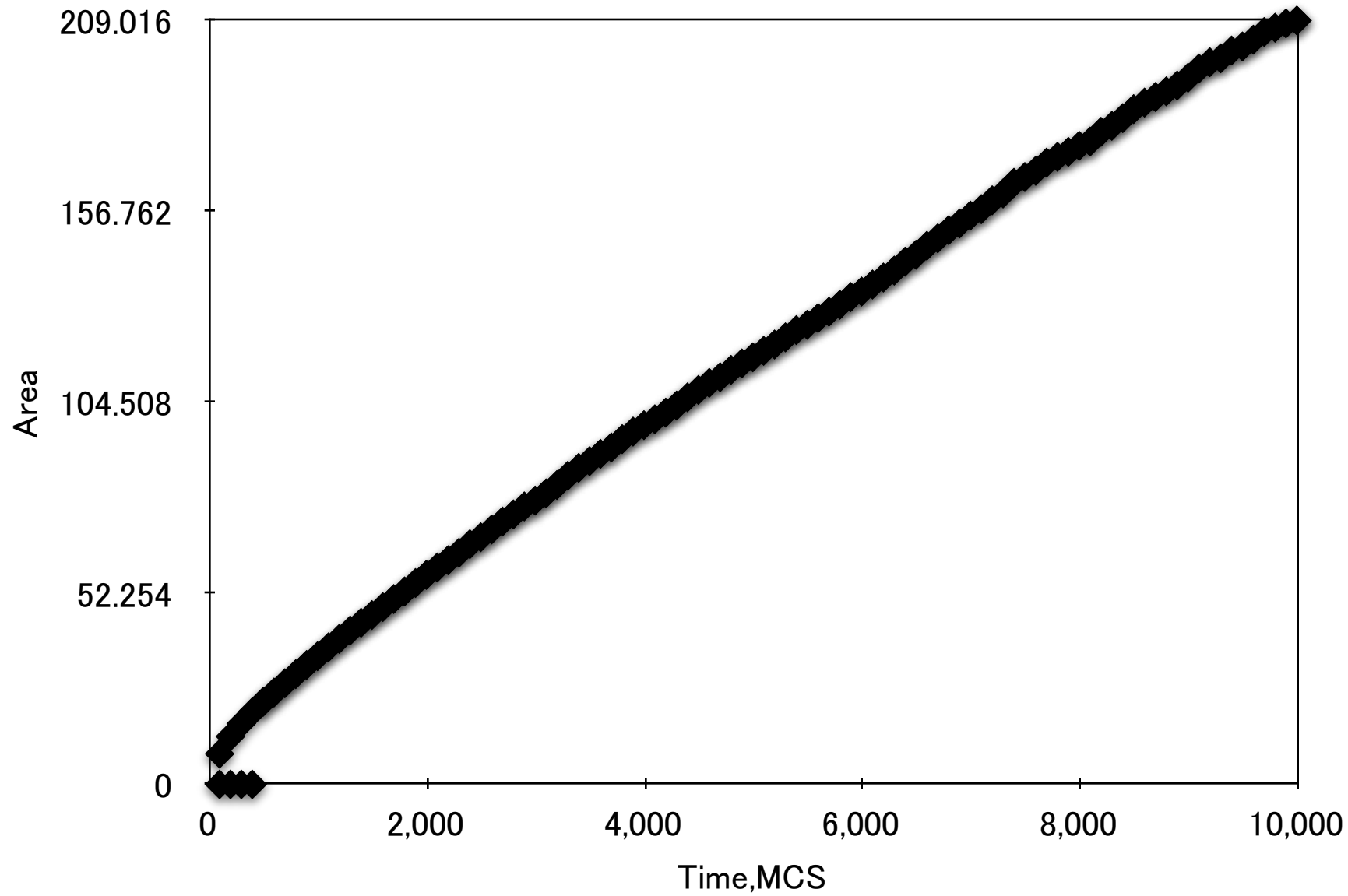
*1000 MCS*

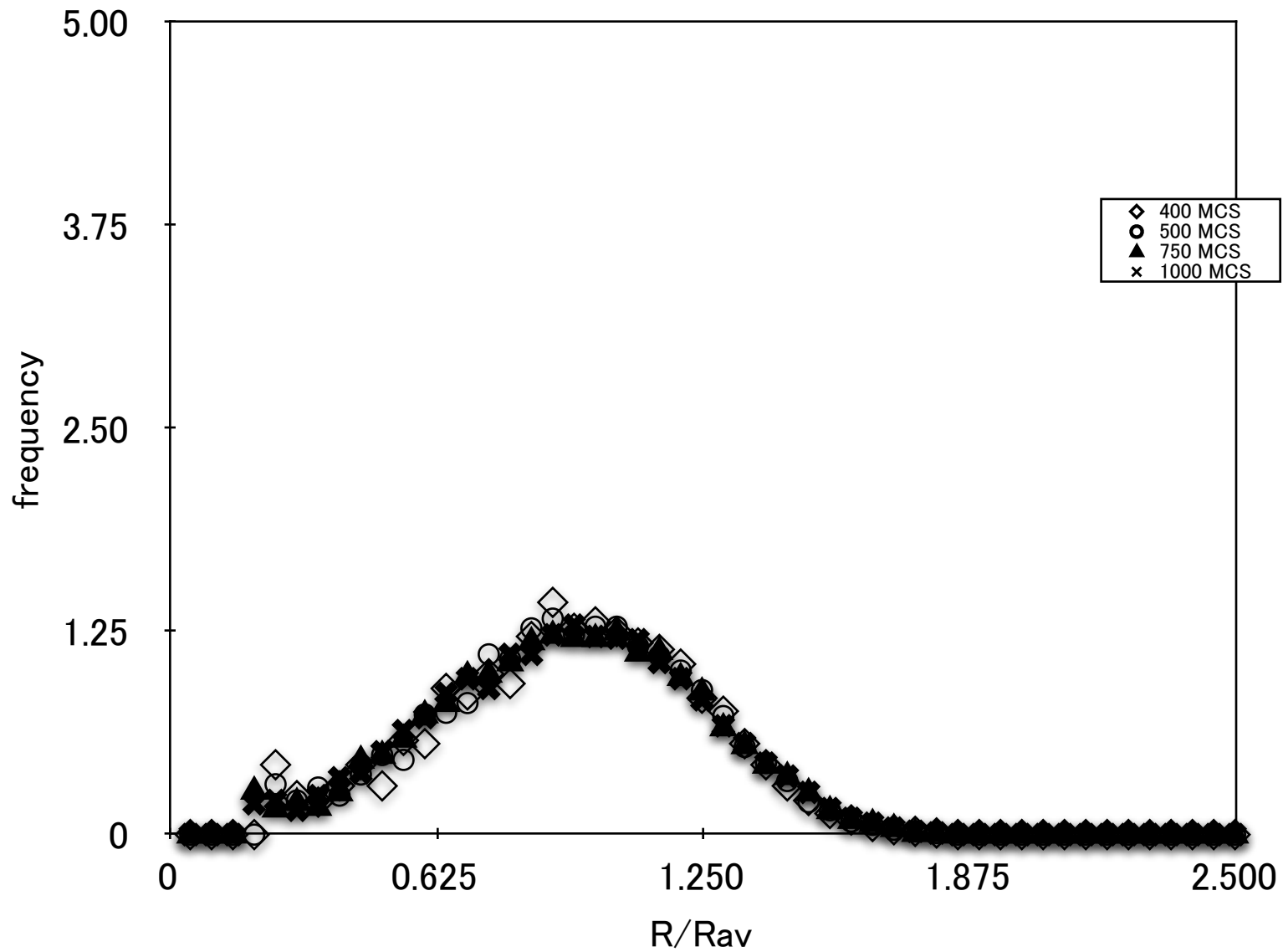


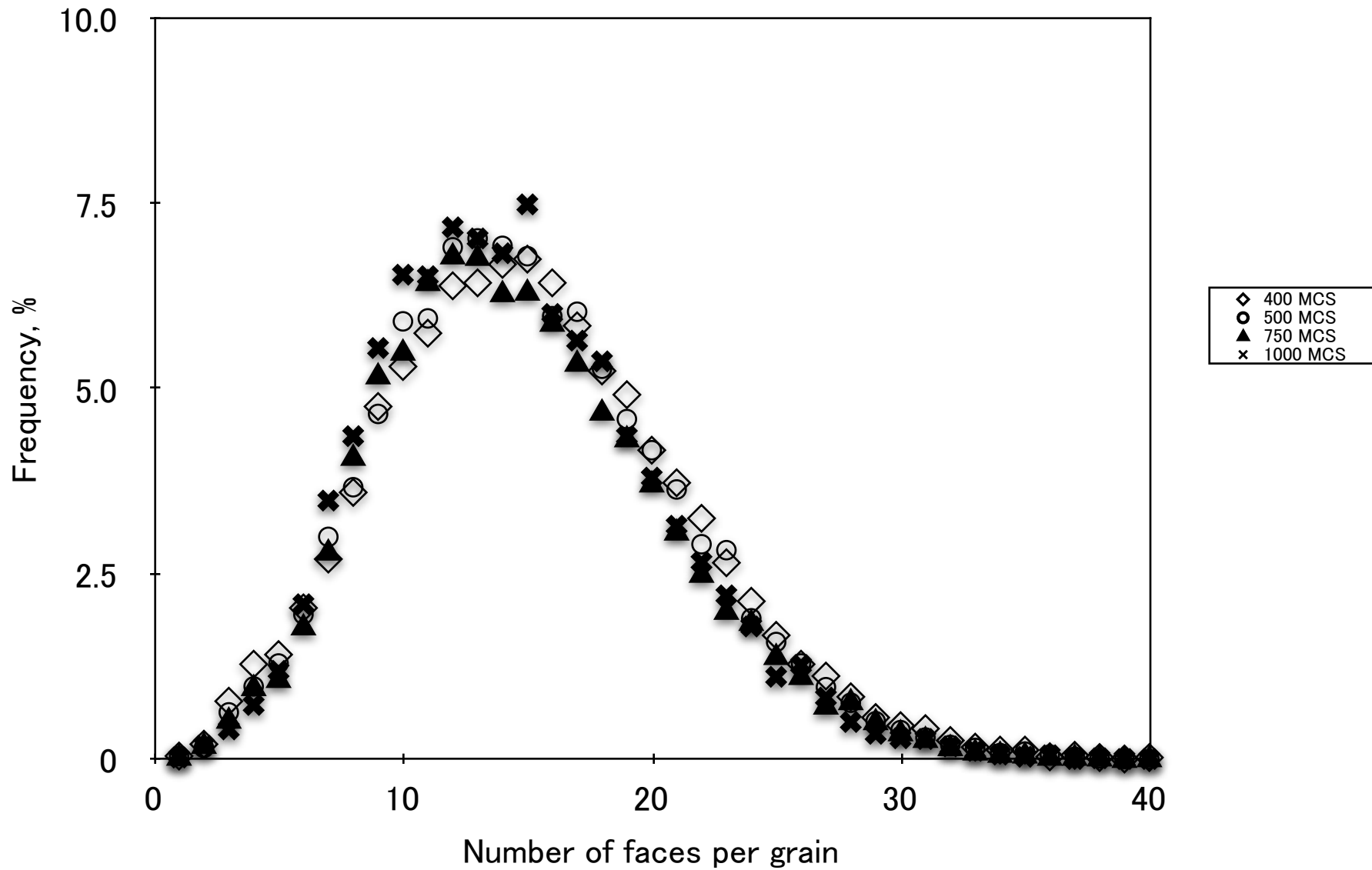
*2000 MCS*

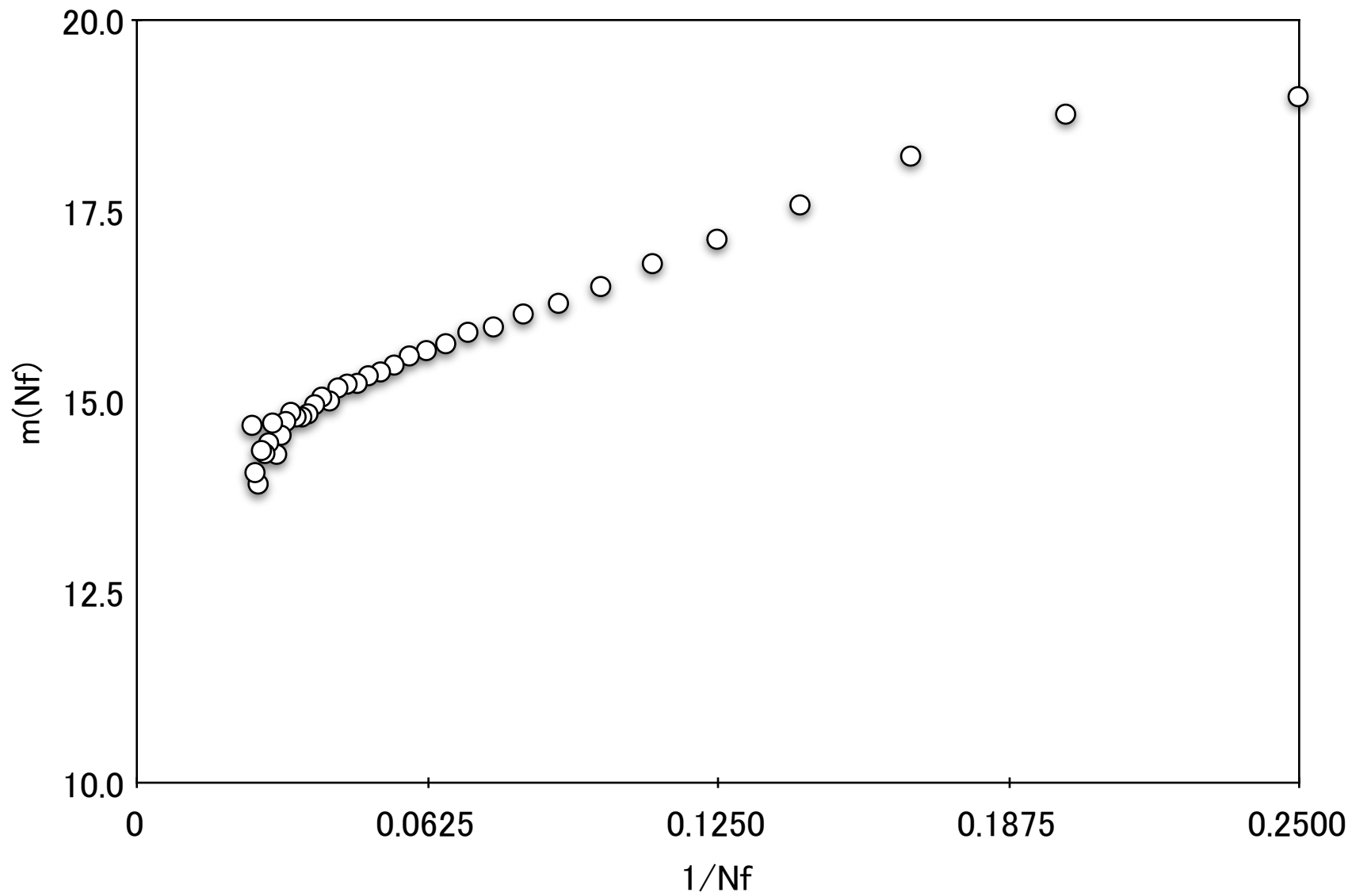


*5000 MCS*



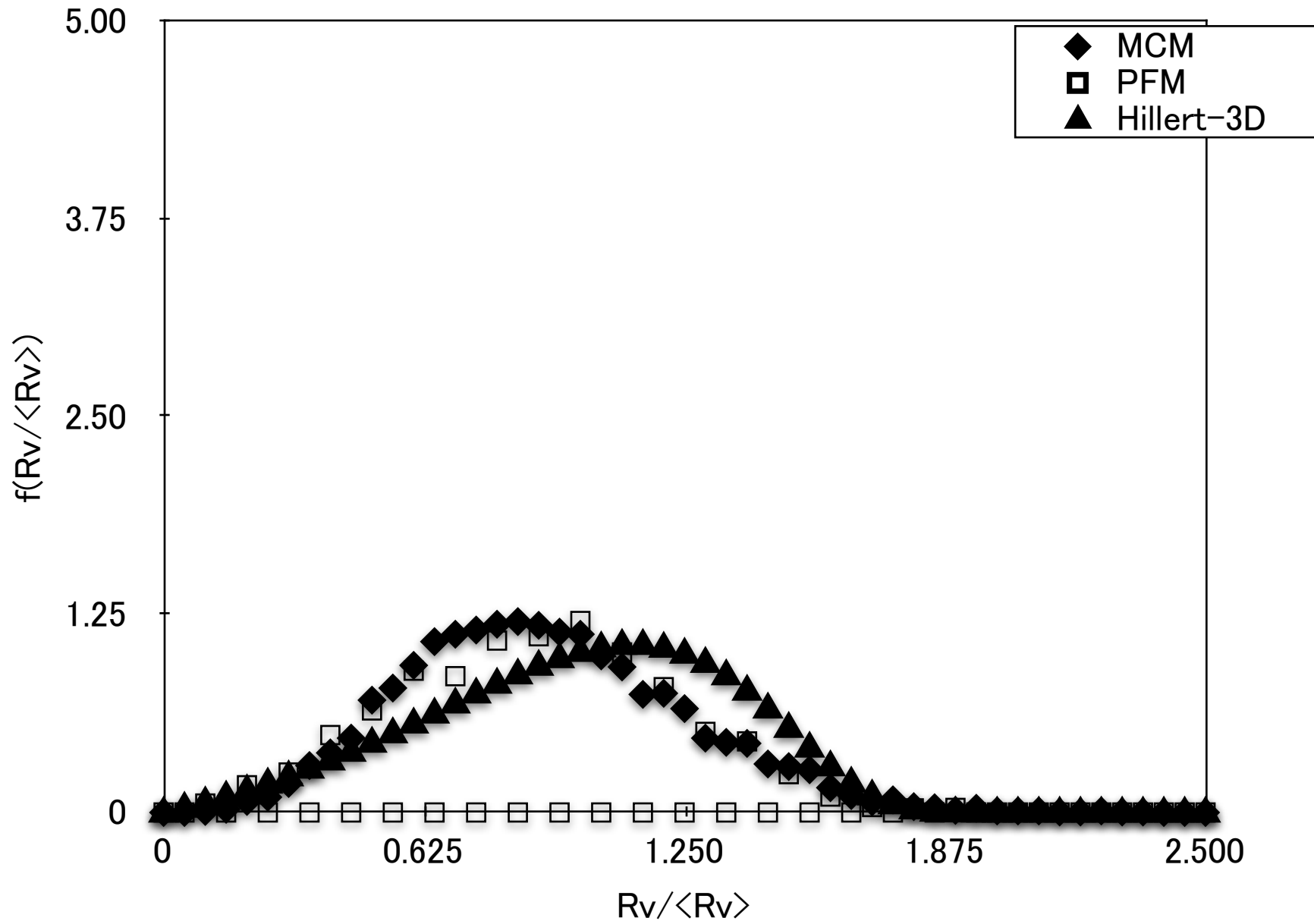


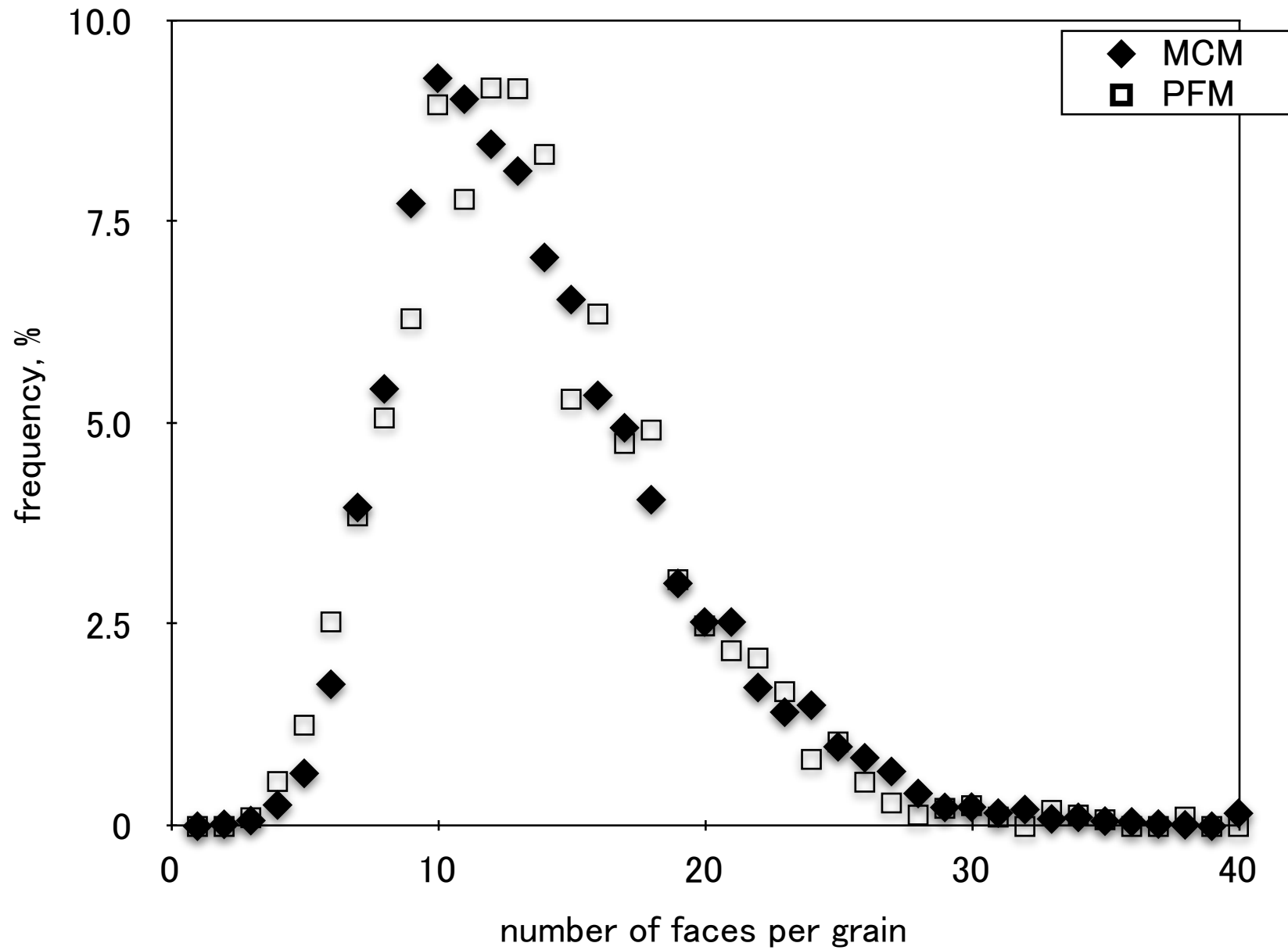


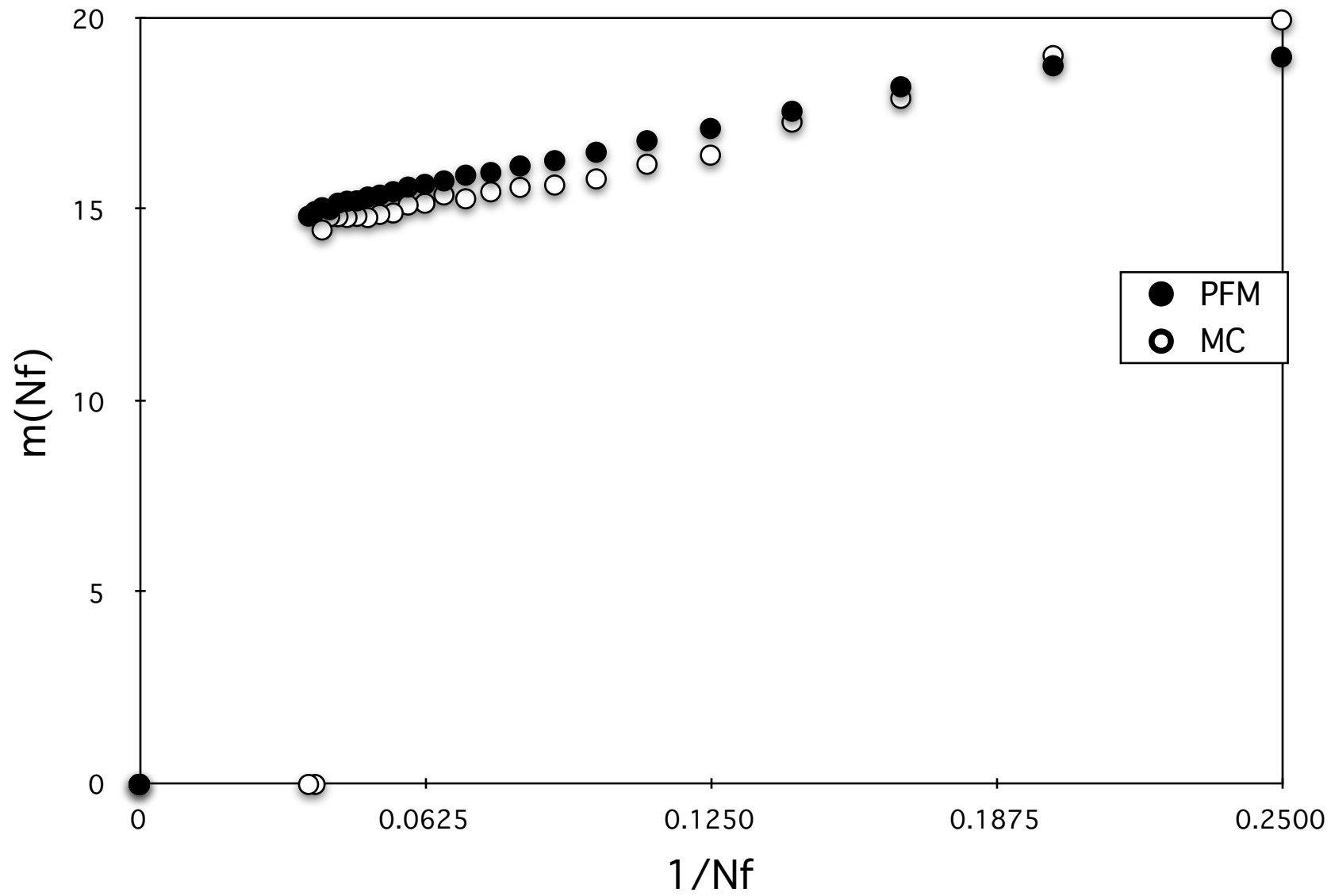


# Phase Field vs. Monte Carlo

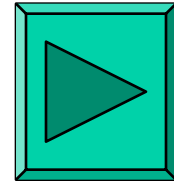








# Phase Field vs. Monte Carlo



# **Problems related to interface migration**

**Effect of anisotropy on grain growth**

**Abnormal grain growth**

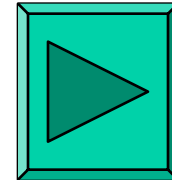
**Effect of second phase**

**Texture control**

**Solute drag effect**

**Recrystallization**

**Phase transformation**



# **Spinodal Decomposition**

# • **Background**

## • **Duplex stainless steel**

- **• high strength, • good weldability, • high resistance to stress corrosion cracking → Chemical reactor**

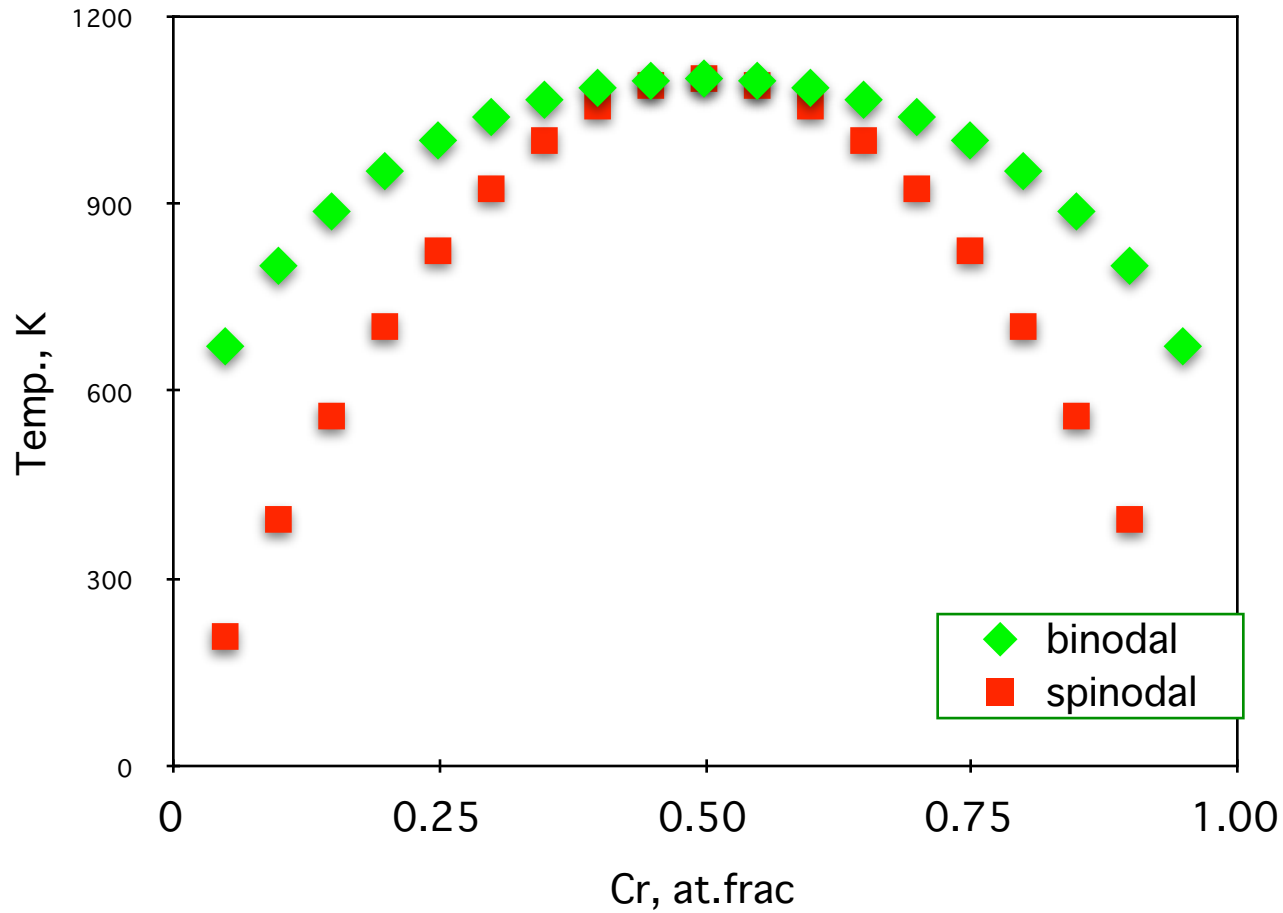
• Problem: 475°C embrittlement

• **Hardening due to thermomechanical instability of ferrite phase in duplex stainless steels**

• **Prediction of long time stability of**

• **chemical reactor**

# Fe-Cr binary alloy





# A numerical method for solving Cahn-Hilliard Equation

$$\frac{C(\vec{r}, t + \Delta t) - C(\vec{r}, t)}{\Delta t} = \frac{M}{(\Delta r)^2} \sum_{NN} \left[ \frac{\partial f_0}{\partial C} - \frac{K}{(\Delta r)^2} \sum_{NN} C(\vec{r}, t) \right]$$

# Second order differential parameter

1D

2D

3D

# Second order differential parameter

1D

$$\sum_{NN} F(x, t) = F(x + \Delta x, t) + F(x - \Delta x, t) - 2F(x, t)$$

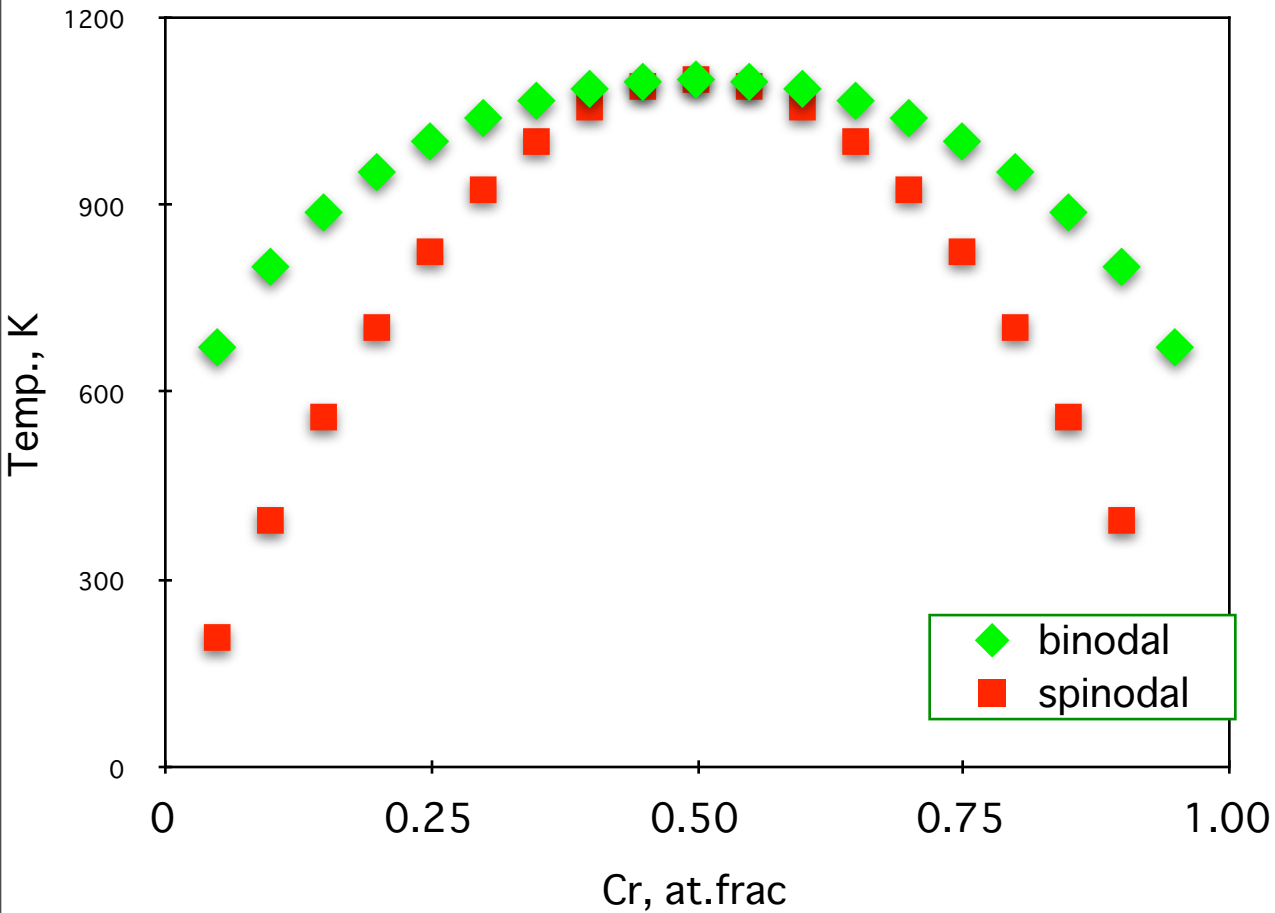
2D

$$\begin{aligned} \sum_{NN} F(x, y, t) = & F(x + \Delta x, y, t) + F(x - \Delta x, y, t) \\ & + F(x, y + \Delta y, t) + F(x, y - \Delta y, t) \\ & - 4F(x, y, t) \end{aligned}$$

3D

$$\begin{aligned} \sum_{NN} F(x, y, z, t) = & F(x + \Delta x, y, z, t) + F(x - \Delta x, y, z, t) \\ & + F(x, y + \Delta y, z, t) + F(x, y - \Delta y, z, t) \\ & + F(x, y, z + \Delta z, t) + F(x, y, z - \Delta z, t) \\ & - 6F(x, y, z, t) \end{aligned}$$

# Fe-Cr binary alloy



## Chemical free energy

$$f_0 = \Omega x(1-x) + RT[x \ln(x) + (1-x) \ln(1-x)]$$

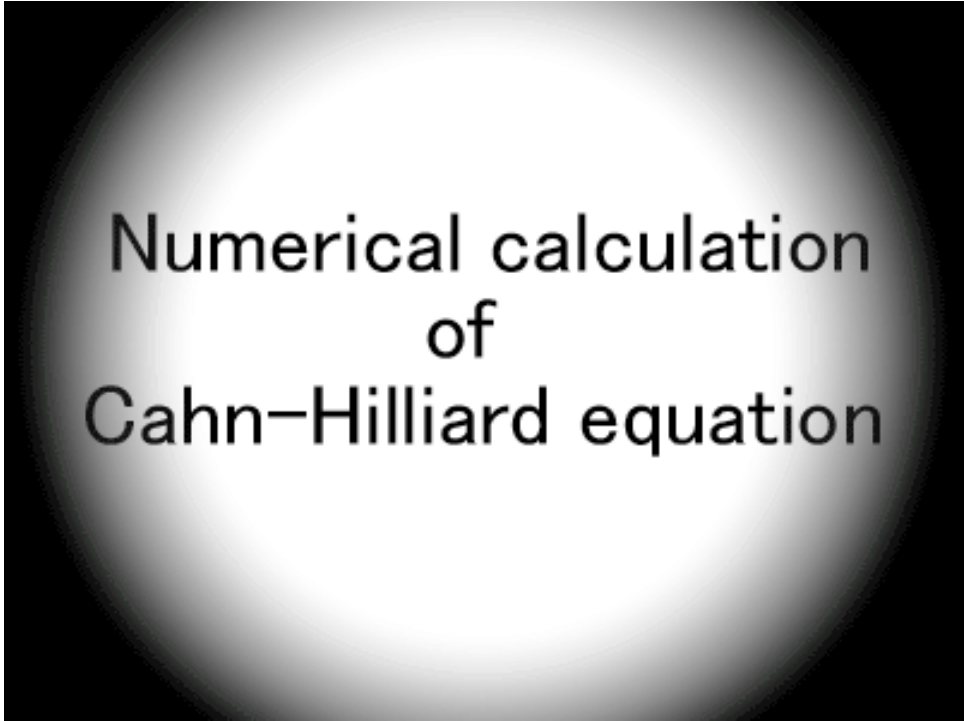
## Phase boundary

$$\frac{\partial f_0}{\partial x} = \dot{U}(1 - 2x) + RT[\ln x - \ln(1 - x)] = 0$$

Spinodal

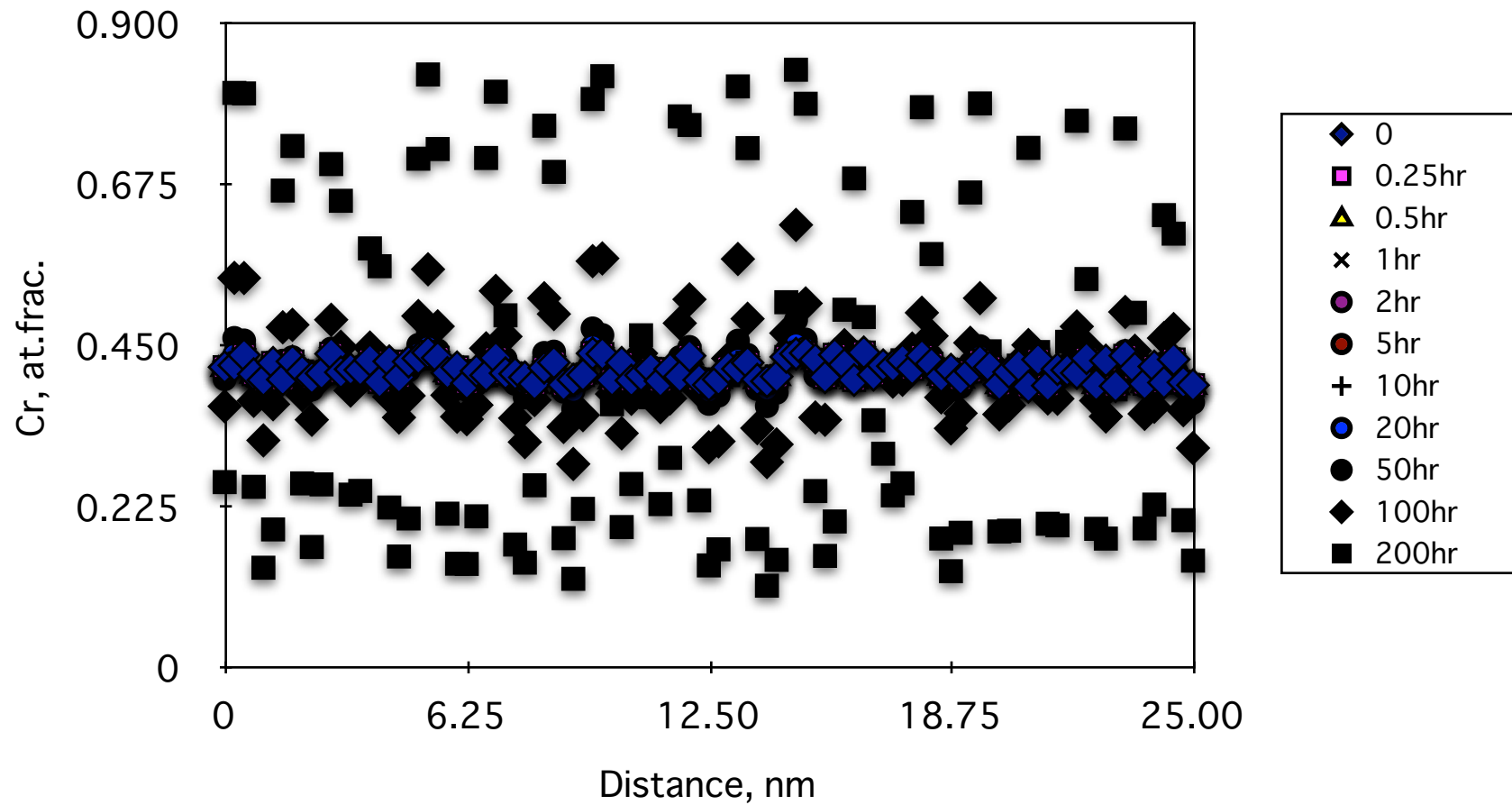
$$\frac{\partial^2 f_0}{\partial x^2} = -2\Omega + RT \left[ \frac{1}{x} + \frac{1}{1-x} \right] = 0$$

Proto type simulation(Fe-40wt.%Cr ally)  
850K



Numerical calculation  
of  
Cahn-Hilliard equation

# Fe-40%Cr binary alloy



# **Simulation of Phase Separation**



# Cahn-Hillirad equation for Fe-X-Y ternary alloys

## Cahn-Hillrad equation for Fe-X-Y ternary alloys

$$\frac{\partial c_X}{\partial t} = M_X \left[ \nabla^2 \left( \frac{\partial f_0}{\partial c_X} - K_X \nabla^2 c_X - L_{XY} \nabla^2 c_Y \right) \right]$$

$$\frac{\partial c_Y}{\partial t} = M_Y \left[ \nabla^2 \left( \frac{\partial f_0}{\partial c_Y} - L_{YX} \nabla^2 c_X - K_Y \nabla^2 c_Y \right) \right]$$

# Condition

Aging temperature  $T$ :

Composition :

Mobility,  $M$  :

**Energy gradient coefficient**

**$K$  :**

**$L$  :**

# Condition

Aging temperature  $T$ : **800**

**K**

Composition :

**Fe-40at.%Cr-5at.%Mo**   **Fe-40at.%Mo-5at.%Cr**

Mobility,  $M$  :  $M_{\text{Cr}} = \frac{0.01 \times D_{\text{Cr}}}{2\Omega_{\text{FeCr}} - 4RT}$     $M_{\text{Mo}} = \frac{0.01 \times D_{\text{Mo}}}{2\Omega_{\text{FeMo}} - 4RT}$

Energy gradient coefficient

$K$  :  $K_{\text{Cr}} = \frac{1}{2} \times a_0^2 \times \Omega_{\text{FeCr}}$     $K_{\text{Mo}} = \frac{1}{2} \times a_0^2 \times \Omega_{\text{FeMo}}$

$L$  :  $L_{\text{CrMo}} = L_{\text{MoCr}} = \frac{1}{2} \times a_0^2 \left( \Omega_{\text{CrMo}} - \Omega_{\text{FeCr}} - \Omega_{\text{FeMo}} \right)$

**Diffusion coefficient  $D$  :**

**Interaction parameter  $\Omega$  :**

## Diffusion coefficient $D$ :

$$D_{\text{Cr}} = 0.19 \exp\left(-\frac{246000}{RT}\right) \text{cm}^2 / \text{s}$$

$$D_{\text{Mo}} = 0.29 \exp\left(-\frac{264000}{RT}\right) \text{cm}^2 / \text{s}$$

## Interaction parameter $\Omega$ :

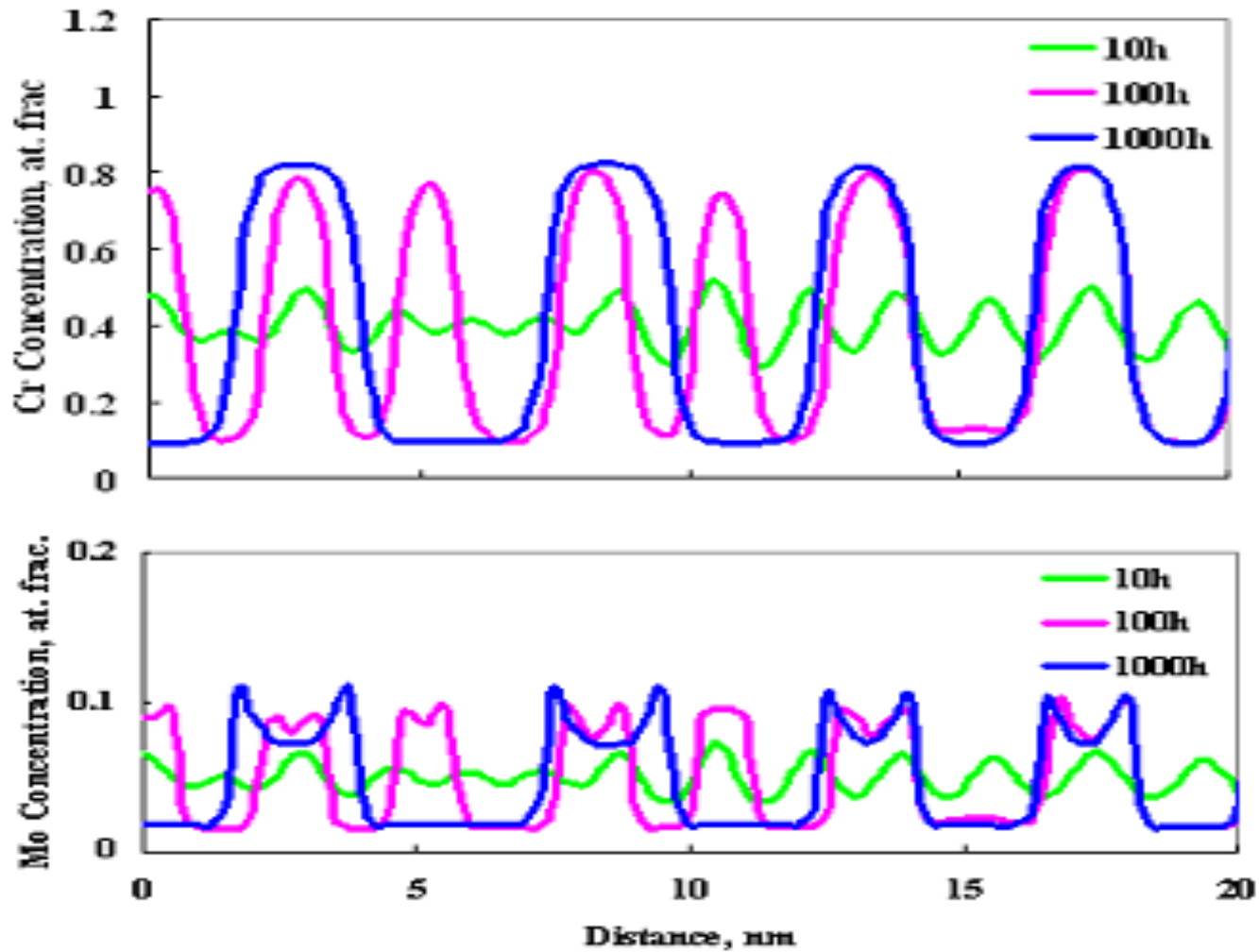
$$\Omega_{\text{FeCr}} = 18.6 \text{kJ/mol}$$

$$\Omega_{\text{FeMo}} = 18.2 \text{kJ/mol}$$

$$\Omega_{\text{CrMo}} = 8.0 \text{kJ/mol}$$

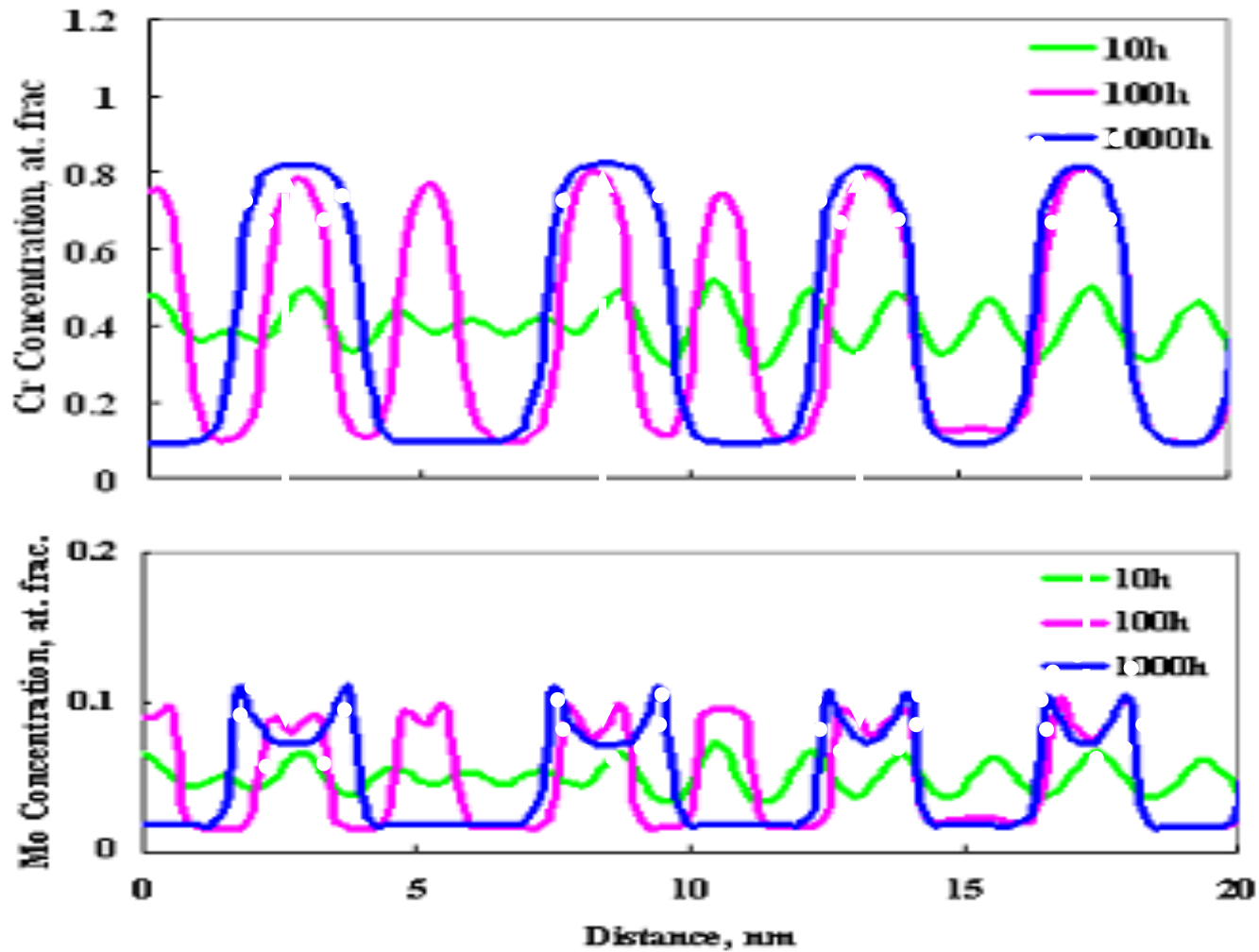
# 1D simulation

Fe<sub>40</sub>Cr<sub>5</sub>Mo(800K)



# 1D simulation

Fe<sub>40</sub>Cr<sub>5</sub>Mo(800K)





# 2D simulation

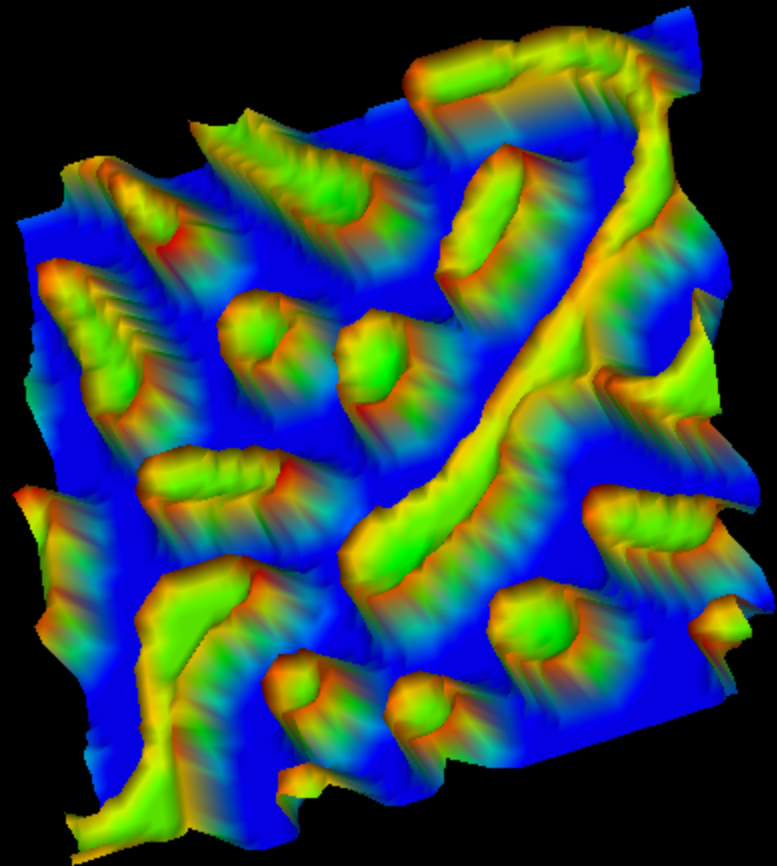
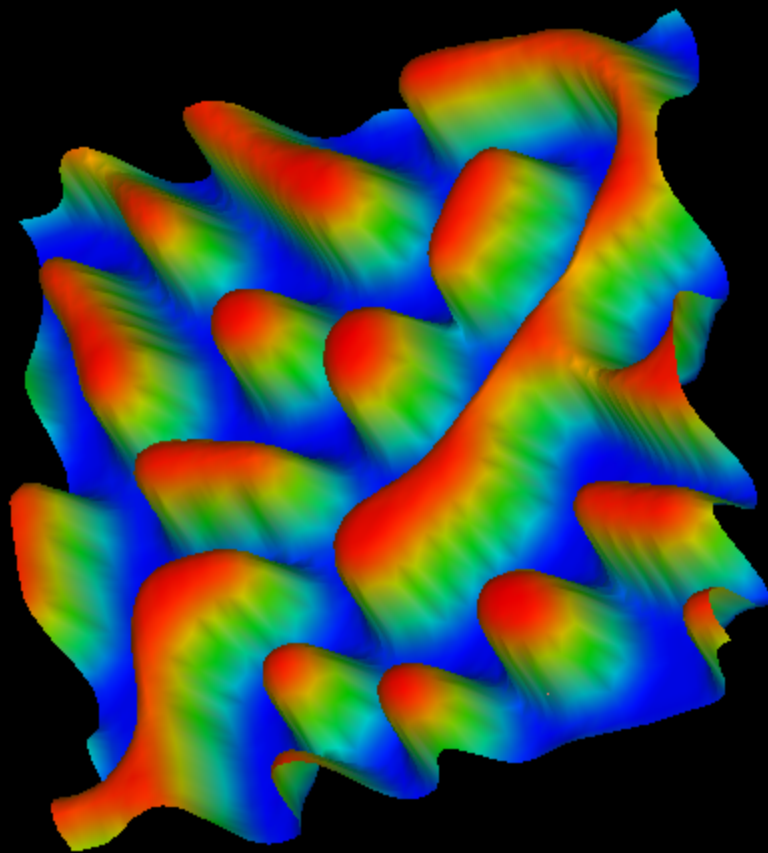
Cr Mo



100

時間後

Fe40Cr5Mo

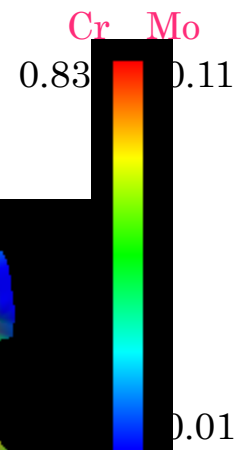


10 μm

Cr

Mo

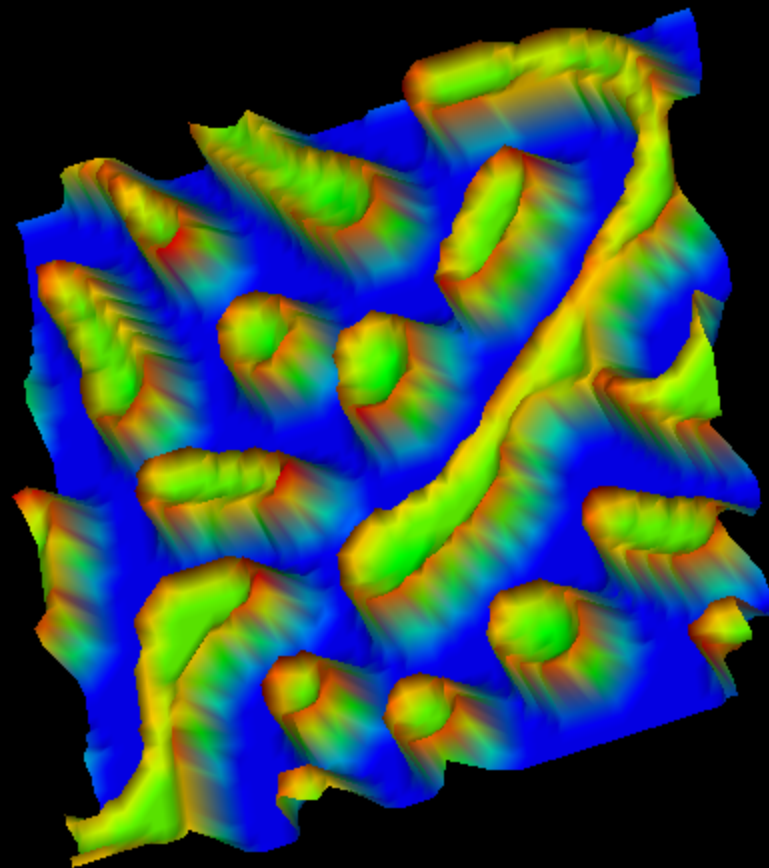
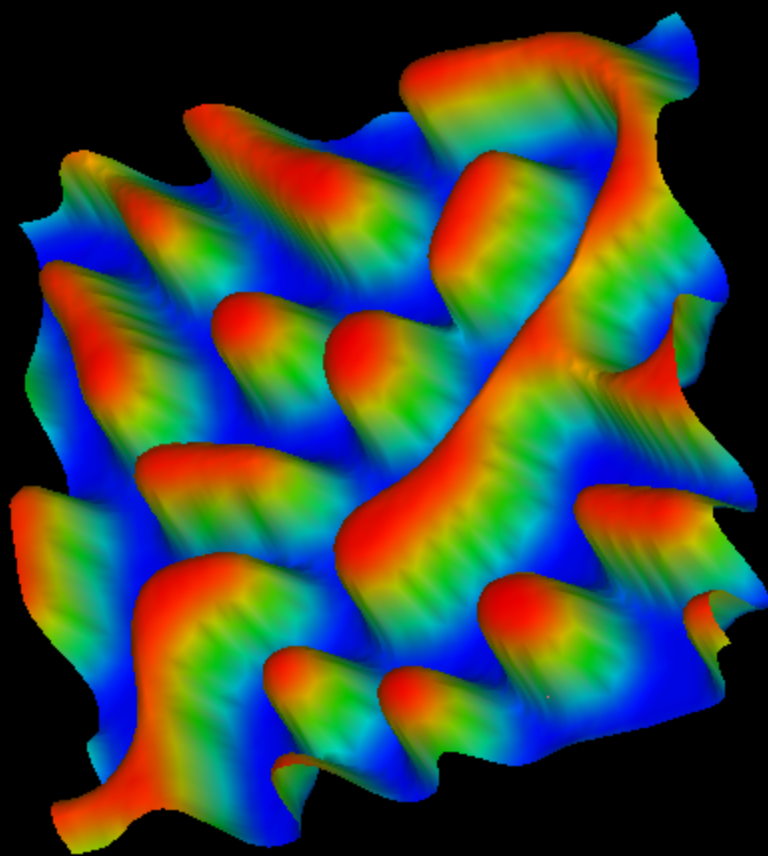
# 2D simulation



100

時間後

Fe40Cr5Mo

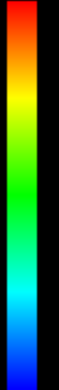


Cr

Mo

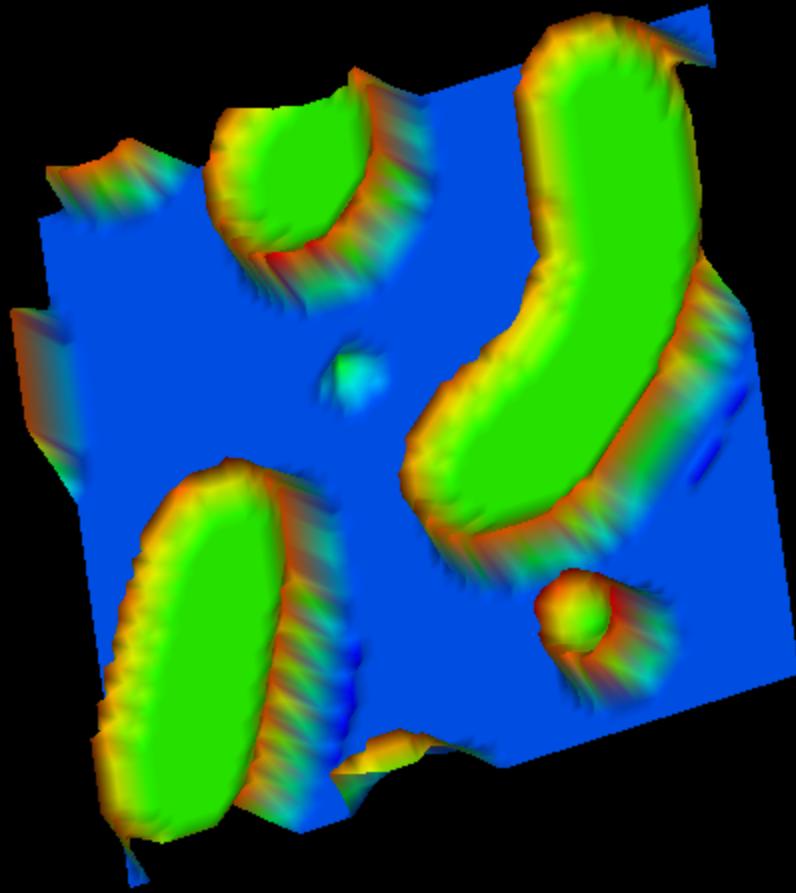
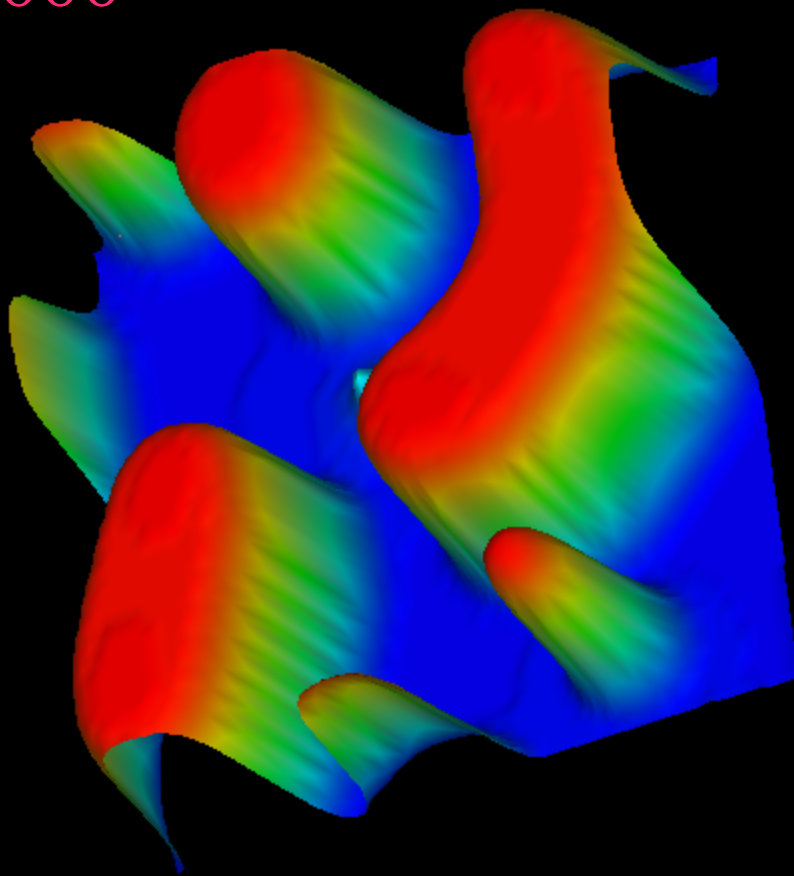
2D

Cr Mo



1000

Cr Mo



16 nm

Cr

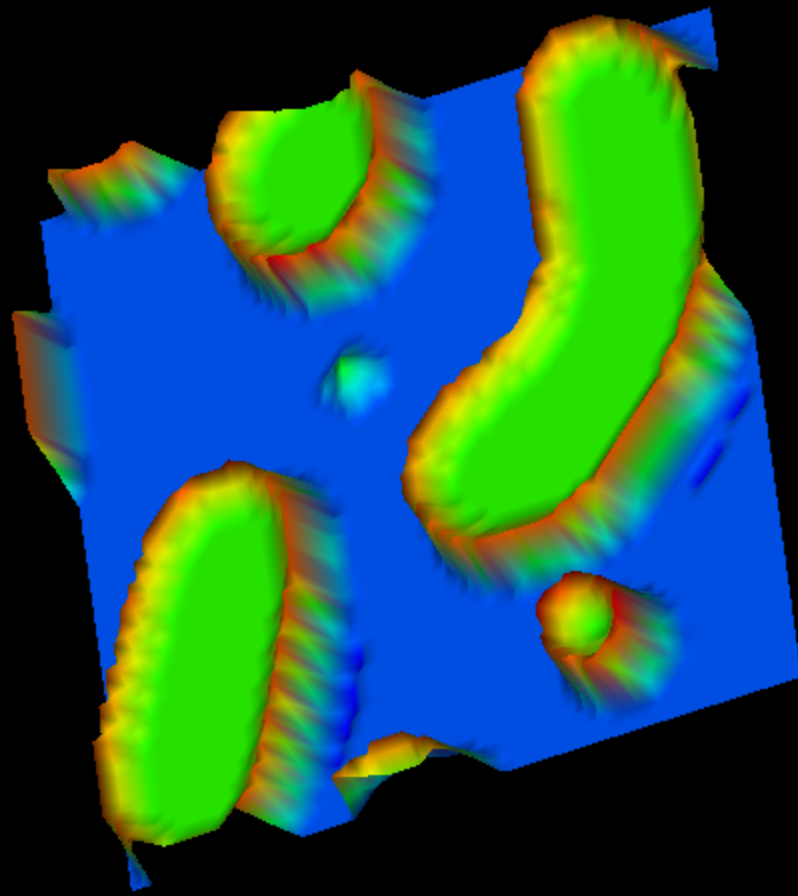
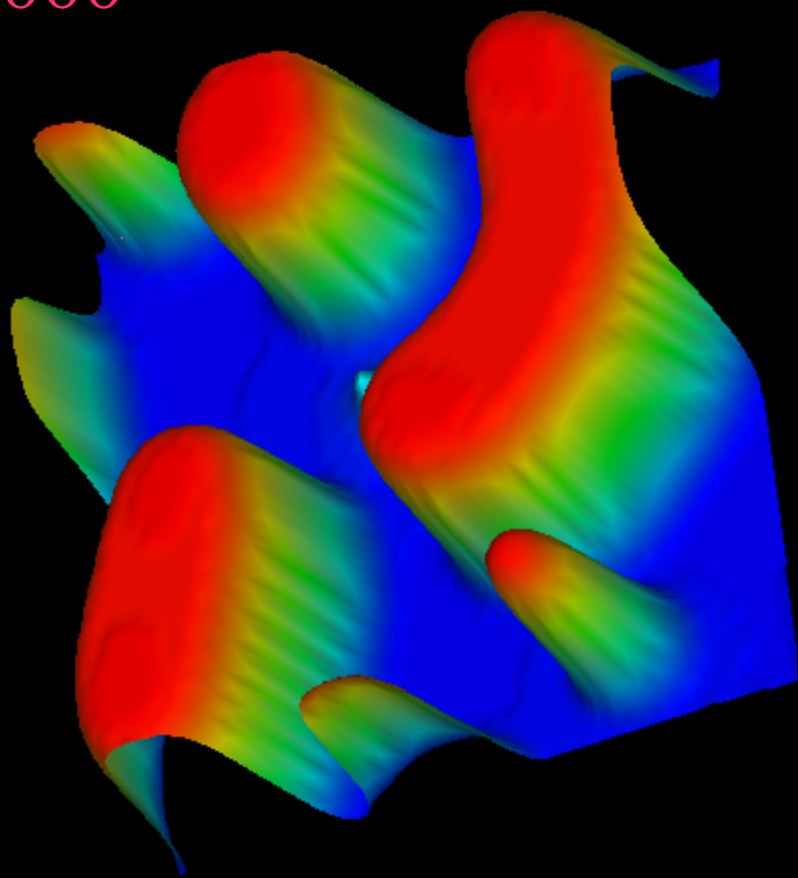
Mo

2D

Cr Mo  
0.82 0.12

1000

Cr Mo

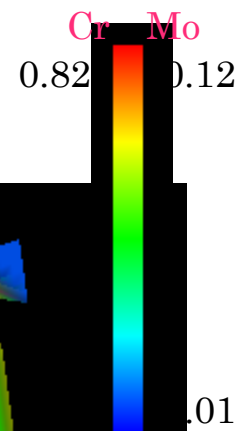


16 nm

Cr

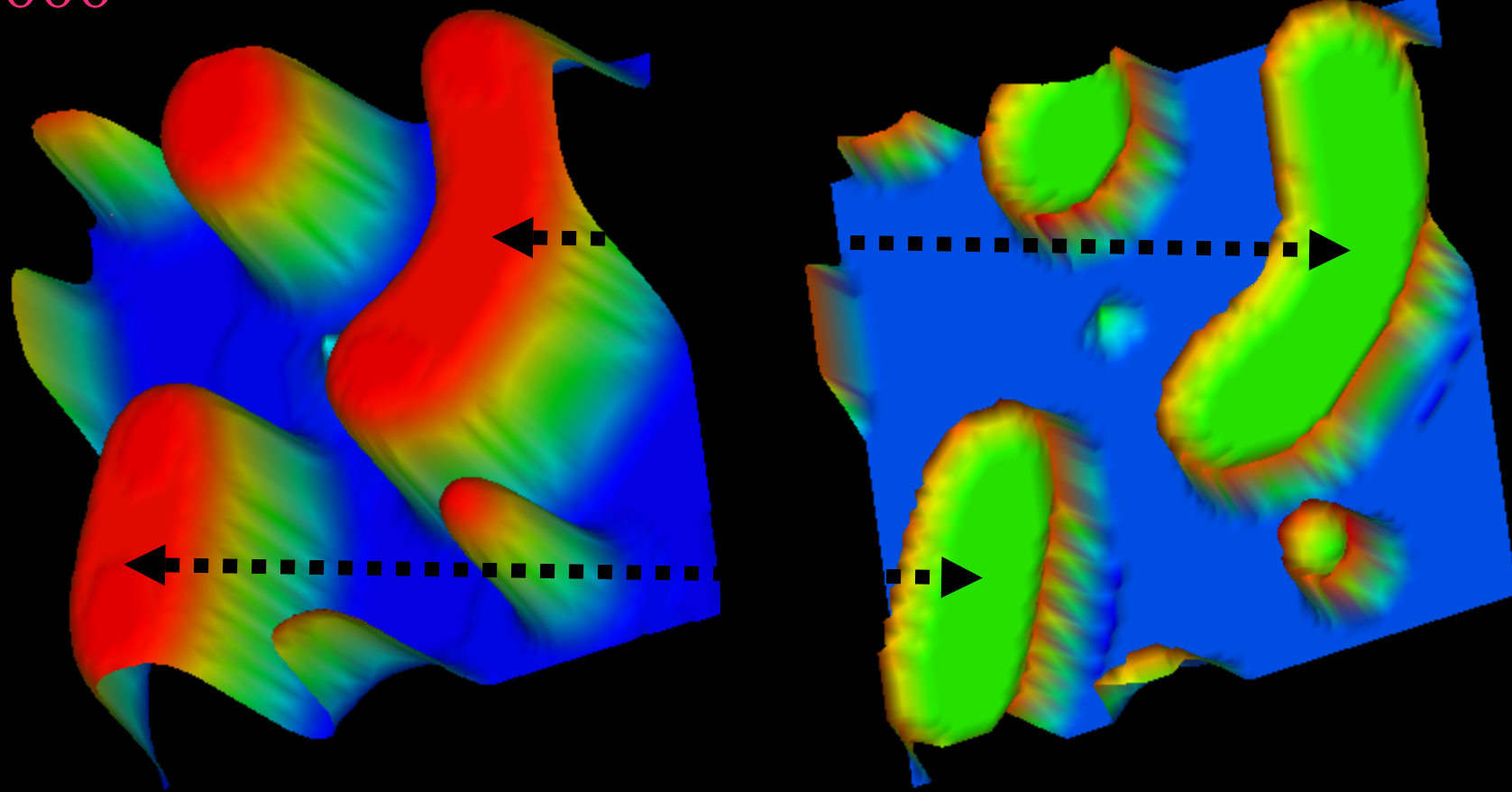
Mo

2D



1000

Cr Mo



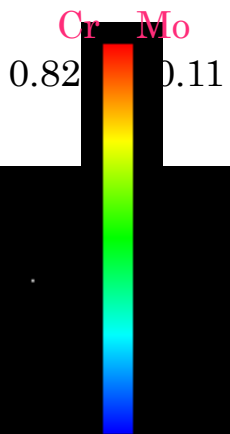
16 nm

Cr

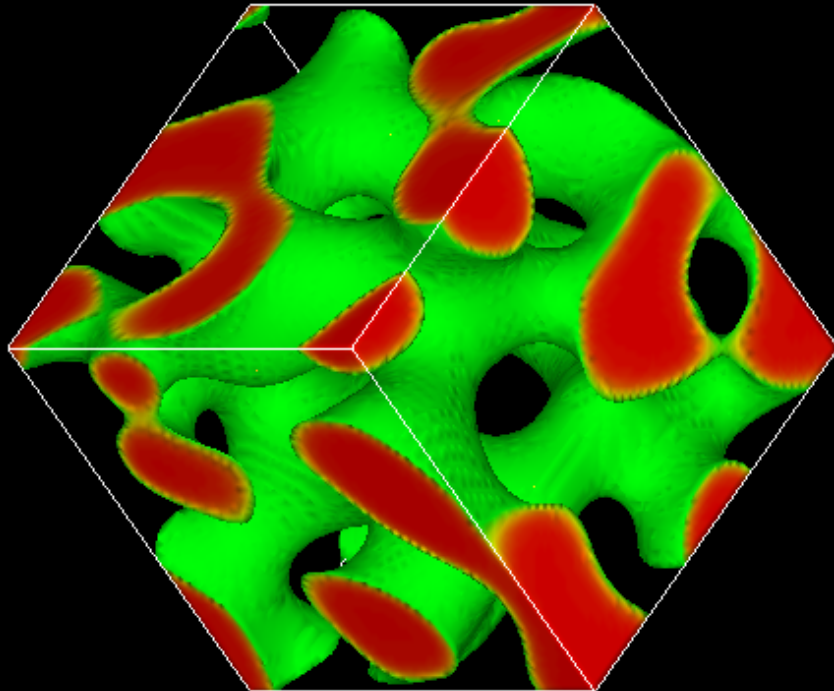
Mo

# 3D simulation

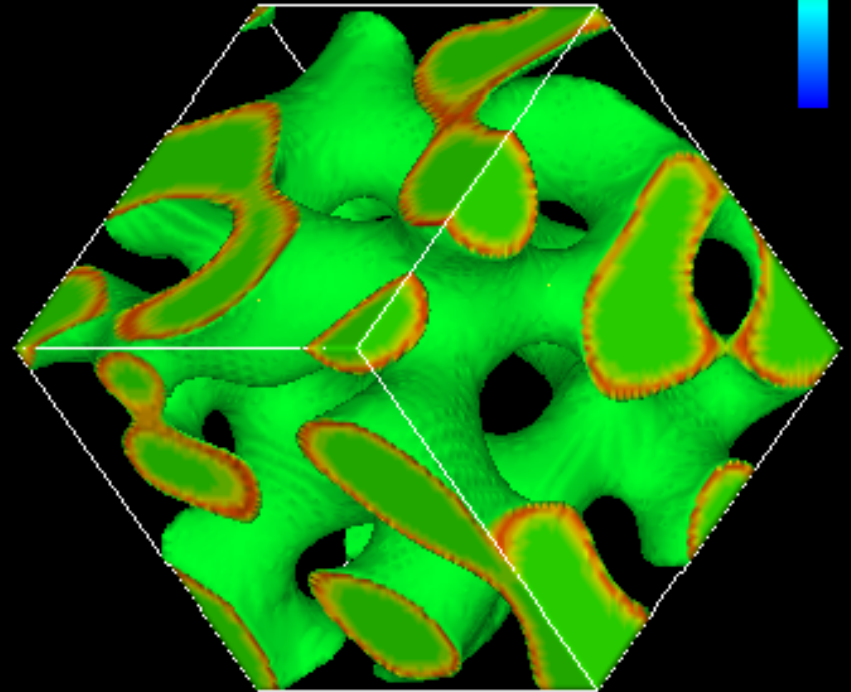
Fe40Cr5Mo



1000



Isosurface of Cr



Isosurface of Mo

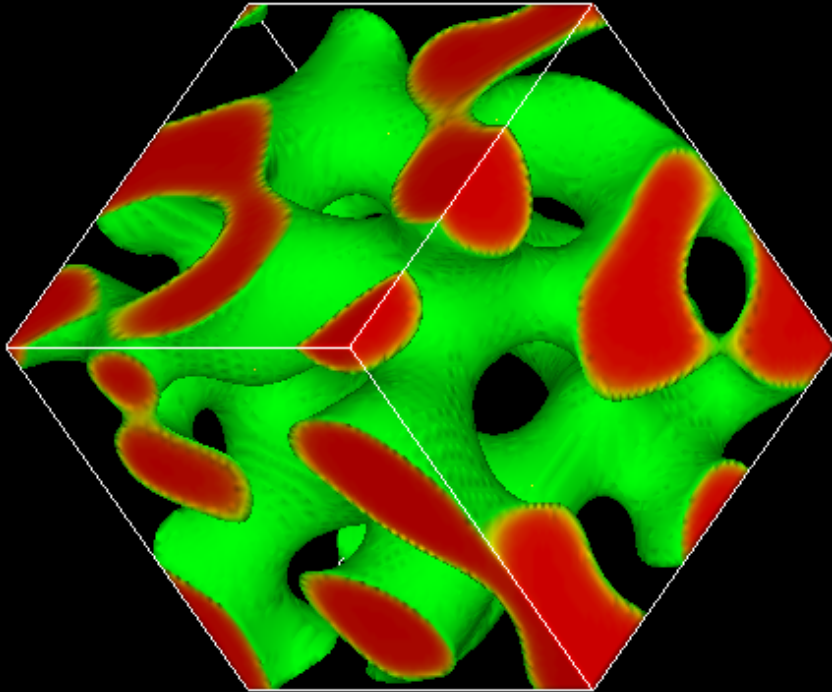


# 3D simulation

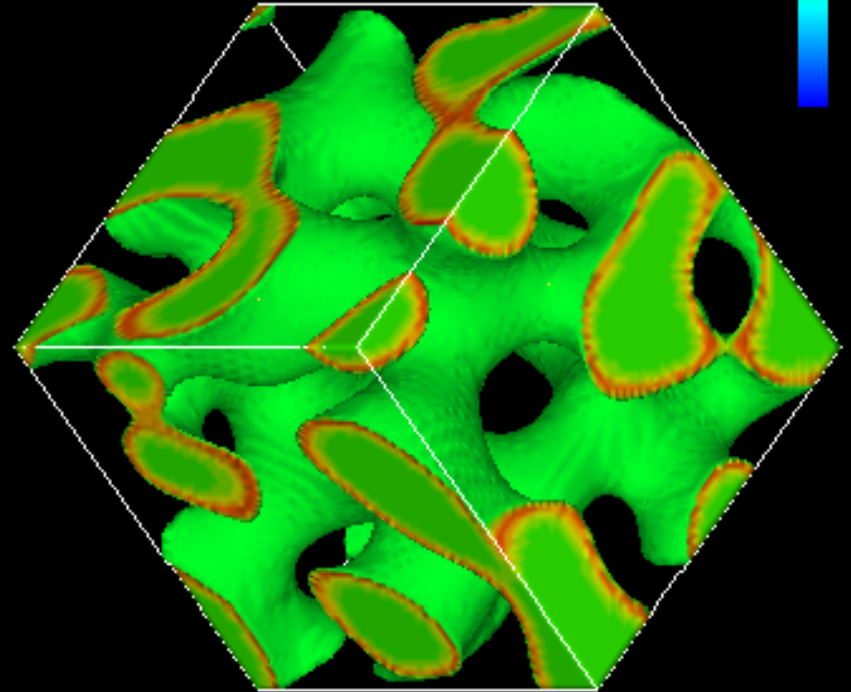
Fe40Cr5Mo



1000

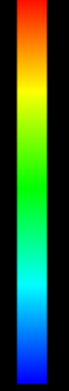


Isosurface of Cr



Isosurface of Mo

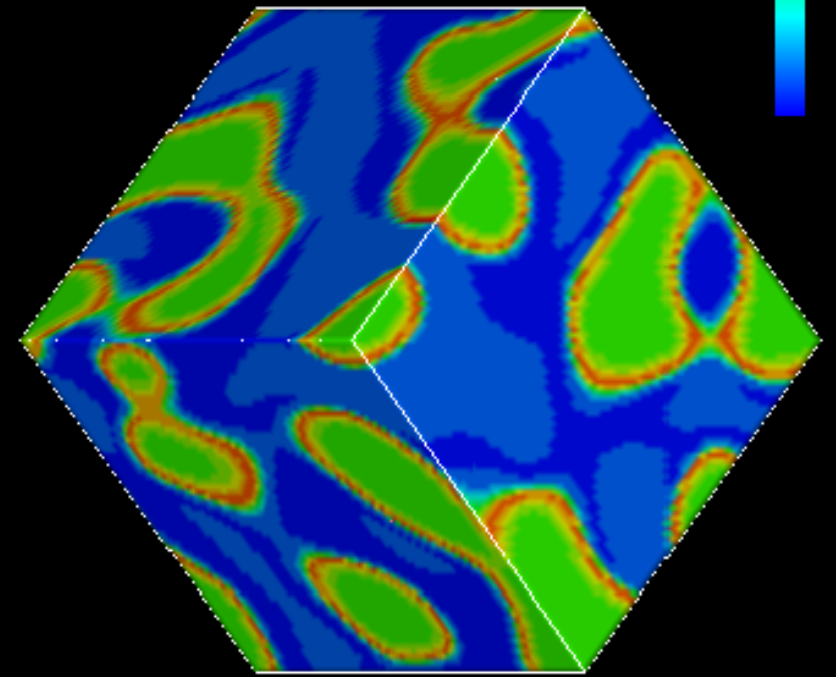
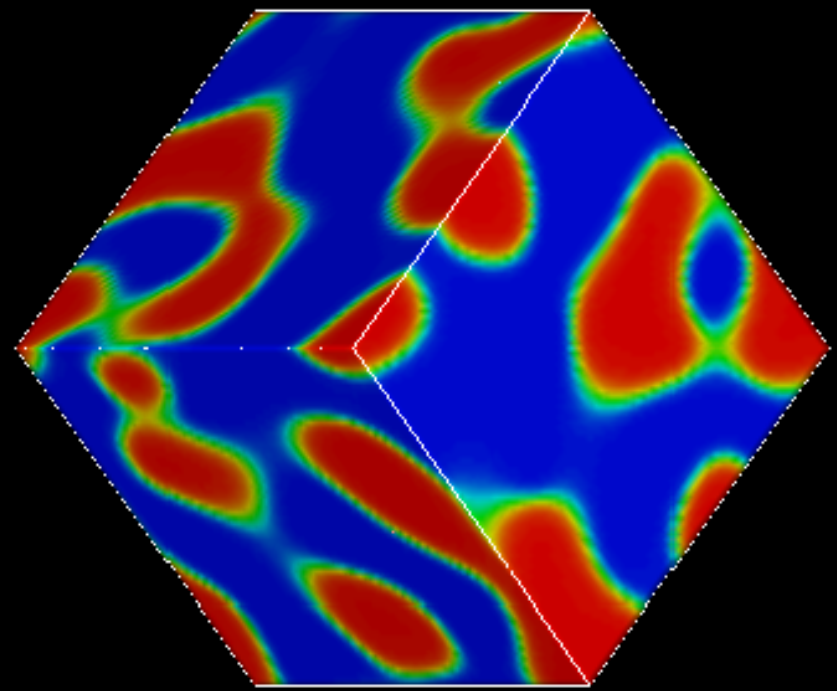
Cr Mo



3D

Cr Mo

1000

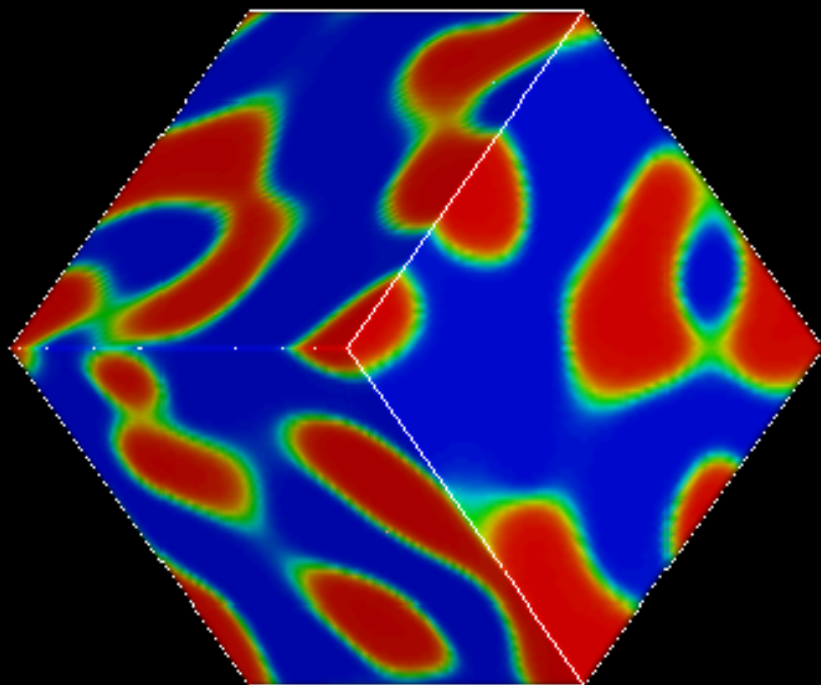


Cr

Mo

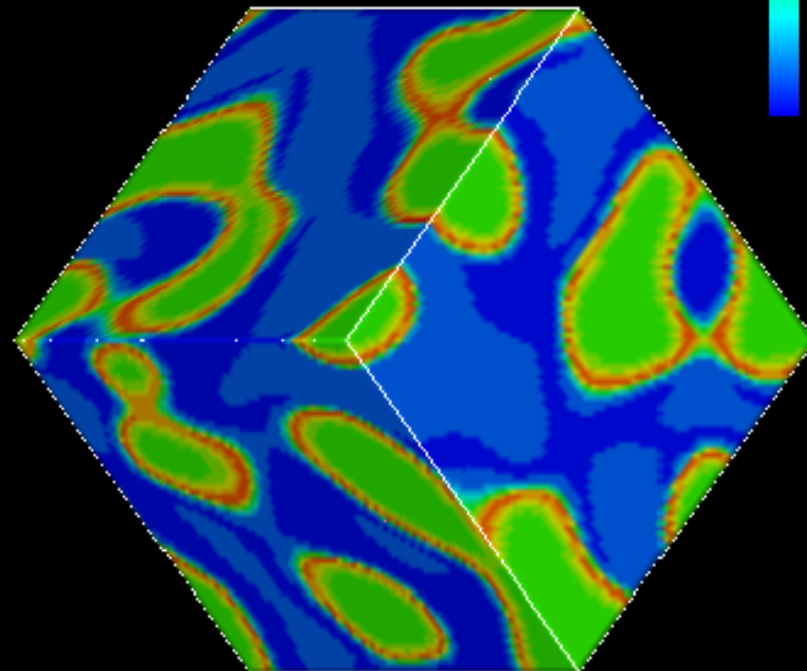


1000

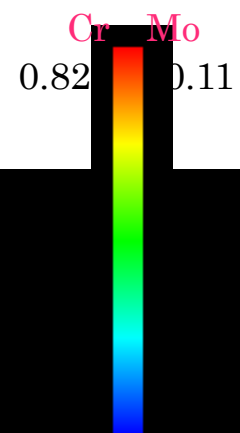


Cr

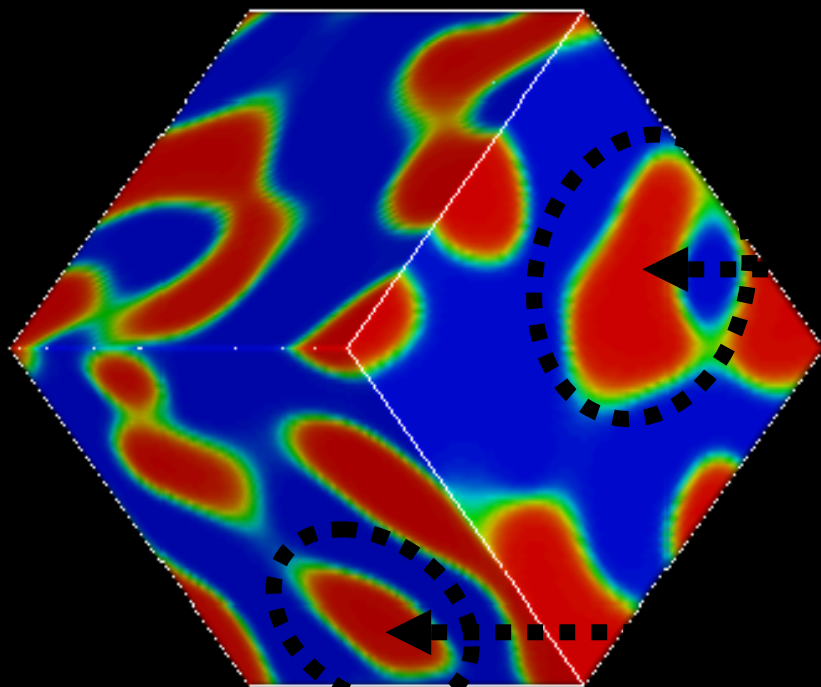
3D  
Cr Mo



Mo

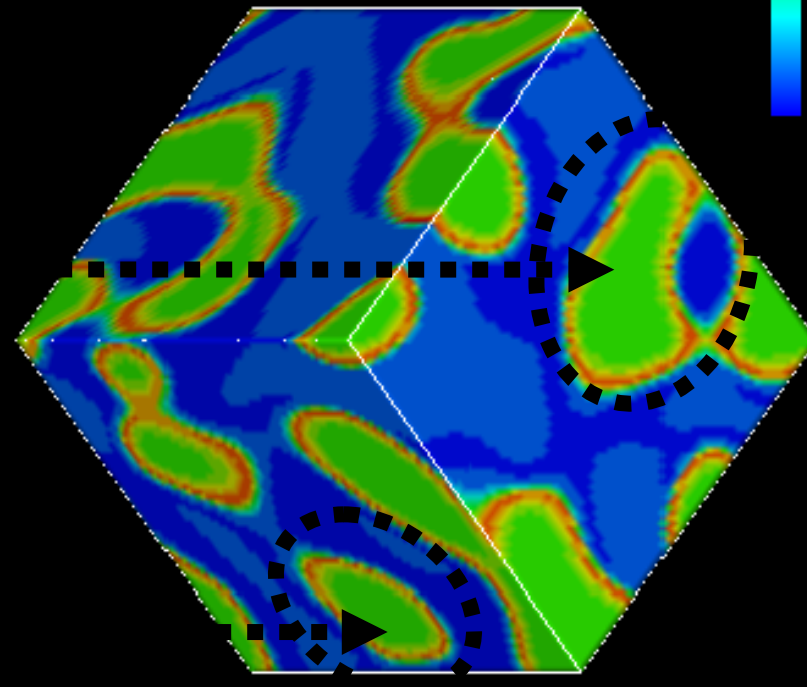


1000

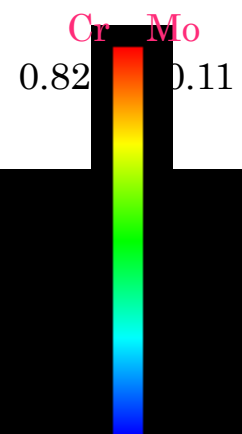


Cr

3D  
Cr Mo



Mo



# **Monte Carlo Simulation**

# Lenard –Jones Parameter

$$e_{ij}(r) = e_{ij}^0 \left[ \left( \frac{r_{ij}}{r} \right)^{12} - 2 \left( \frac{r_{ij}}{r} \right)^6 \right]$$

$r_{ij}$  : equilibrium atomic spacing

$-e_{ij}^0$

Interatomic potential at equilibrium atomic spacing

# Lenard-Jones potentila

$$e_{ij}(r) = e_{ij}^0 \left[ \left( \frac{r_{ij}}{r} \right)^{12} - 2 \left( \frac{r_{ij}}{r} \right)^6 \right]$$

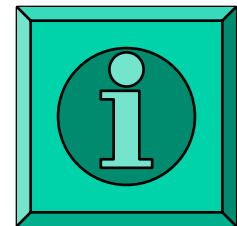
## Normalized Lenard-Jones parameter

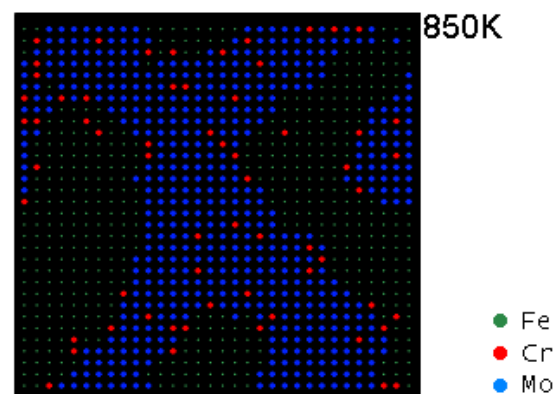
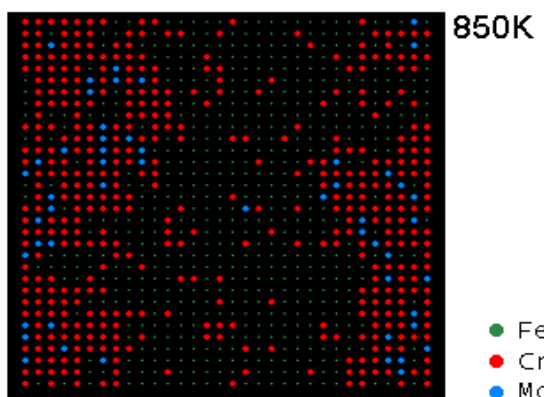
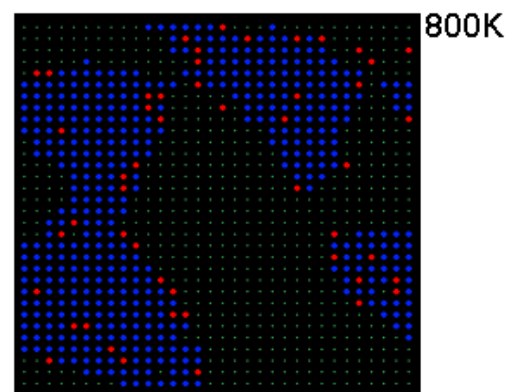
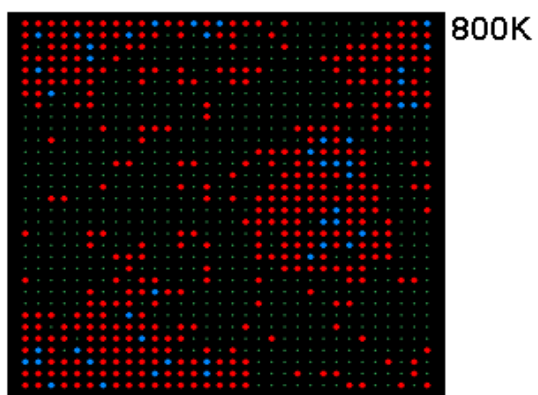
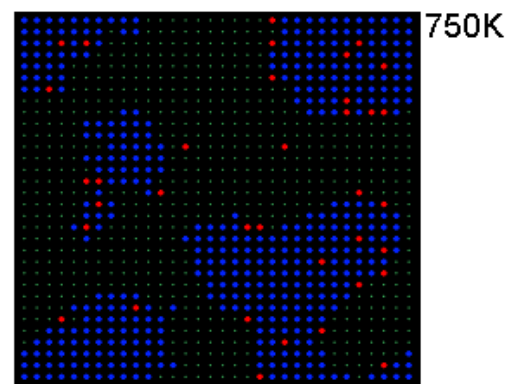
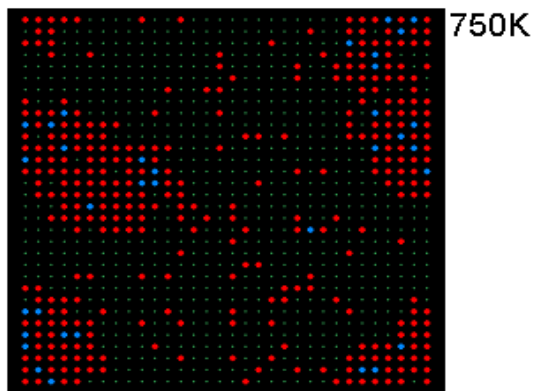
$e_{FeFe}$	$e_{FeCr} / e_{FeFe}$	$e_{FeMo} / e_{FeFe}$	$e_{CrCr} / e_{FeFe}$	$e_{CrMo} / e_{FeFe}$	$e_{MoMo} / e_{FeFe}$
62.0 KJ/ mol	0.9537	1.2296	0.9809	1.3001	1.6390

## Condition

Fe-40at.%Cr-5at.%Mo	750K
Fe-40at.%Mo-5at.%Cr	800K
	850K

# Monte Carlo Simulation





Separation of peaks of Mo



# Behavior of element Y along the trajectory of peak top of element X

$$\frac{d c_Y}{d t} (x_p, t) \cong M_Y \frac{\partial^2 f_0}{\partial c_X \partial c_Y} \frac{\partial^2 c_1}{\partial x^2}$$

# Behavior of element Y along the trajectory of peak top of element X

$$\frac{d c_Y}{d t} (x_p, t) \cong M_Y \frac{\partial^2 f_0}{\partial c_X \partial c_Y} \frac{\partial^2 c_1}{\partial x^2}$$

$\frac{\partial^2 c_X}{\partial x^2} < 0$

# Regular solution model

$$\mathbf{f}_0 = \mathbf{f}_{\text{Fe}} \mathbf{c}_{\text{Fe}} + \mathbf{f}_{\text{X}} \mathbf{c}_{\text{X}} + \mathbf{f}_{\text{Y}} \mathbf{c}_{\text{Y}} +$$
$$\Omega_{\text{XY}} \mathbf{c}_{\text{X}} \mathbf{c}_{\text{Y}} + \Omega_{\text{Fe X}} \mathbf{c}_{\text{Fe}} \mathbf{c}_{\text{X}} + \Omega_{\text{Fe Y}} \mathbf{c}_{\text{Fe}} \mathbf{c}_{\text{Y}} +$$
$$\text{RT} \left[ \mathbf{c}_{\text{Fe}} \ln \mathbf{c}_{\text{Fe}} + \mathbf{c}_{\text{X}} \ln \mathbf{c}_{\text{X}} + \mathbf{c}_{\text{Y}} \ln \mathbf{c}_{\text{Y}} \right]$$

$$\mathbf{c}_{\text{Fe}} + \mathbf{c}_{\text{X}} + \mathbf{c}_{\text{Y}} = 1$$

$$\frac{\partial^2 \mathbf{f}_0}{\partial \mathbf{c}_X^2} = -2\Omega_{\text{Fe X}} + \mathbf{RT} \left( \frac{1}{\mathbf{c}_X} + \frac{1}{1 - \mathbf{c}_X - \mathbf{c}_Y} \right) \dots (1)$$

$$\frac{\partial^2 \mathbf{f}_0}{\partial \mathbf{c}_Y^2} = -2\Omega_{\text{Fe Y}} + \mathbf{RT} \left( \frac{1}{\mathbf{c}_Y} + \frac{1}{1 - \mathbf{c}_X - \mathbf{c}_Y} \right) \dots (2)$$

$$\frac{\partial^2 \mathbf{f}_0}{\partial \mathbf{c}_X \partial \mathbf{c}_Y} = \Omega_{\text{XY}} - \Omega_{\text{Fe X}} - \Omega_{\text{Fe Y}} + \mathbf{RT} \frac{1}{1 - \mathbf{c}_X - \mathbf{c}_Y} \dots (3)$$

$$\frac{\partial^2 \mathbf{f}_0}{\partial \mathbf{c}_X^2} = -2\Omega_{\text{Fe X}} + \mathbf{RT} \left( \frac{1}{\mathbf{c}_X} + \frac{1}{1 - \mathbf{c}_X - \mathbf{c}_Y} \right) \dots (1)$$

$$\frac{\partial^2 \mathbf{f}_0}{\partial \mathbf{c}_Y^2} = -2\Omega_{\text{Fe Y}} + \mathbf{RT} \left( \frac{1}{\mathbf{c}_Y} + \frac{1}{1 - \mathbf{c}_X - \mathbf{c}_Y} \right) \dots (2)$$

$$\frac{\partial^2 \mathbf{f}_0}{\partial \mathbf{c}_X \partial \mathbf{c}_Y} = \Omega_{\text{XY}} - \Omega_{\text{Fe X}} - \Omega_{\text{Fe Y}} + \mathbf{RT} \frac{1}{1 - \mathbf{c}_X - \mathbf{c}_Y} \dots (3)$$

# Modelling of microstructural evolution in structural steel

- 1st stage(1985-1995)  
Integrated model based on thermodynamics and phase transformation theory
- 2nd stage(1995-2005)  
MC, PF for Grain growth, Spinodal decomposition etc.
- 3rd stage(2005- )  
Multiscale 3-D simulation for microstructural evolution in structural steel.

## Microscopic model

Thermodynamics model

Kinetic model

→ Prediction of microstructure

+ FEM →

Prediction of mechanical properties

## Mesoscopic model

Phase field model

Monte Carlo method

Neural network

## Mathematical method

# **Dynamics and Microstructure Evolution in Metals during and after the process of Severe Plastic Deformation**

Tetsuya Ohashi (Kitami Institute of Technology),

Mitsutoshi Kuroda (Yamagata University),

Yoshiyuki Saito (Waseda University),

Tadanobu Inoue (National Institute of Material Science)

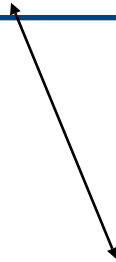
Objectives of this study group are to clarify underlying mechanisms for the development of fine-grained microstructures and to understand the mechanical response of metal polycrystals with high-density lattice defects by using numerical techniques of macro- and meso-mechanics. In the macroscopic analyses, strain histories in materials processed by ARB or ECAP are quantitatively evaluated. The crystal plasticity analyses are performed to understand the characteristics and particularities of dislocation accumulations under different deformation modes. Macroscopic mechanical responses of nano-structured metals are also predicted by crystal plasticity analyses. Thermodynamic stability of ultrafine grained structures is discussed with phase field simulations.

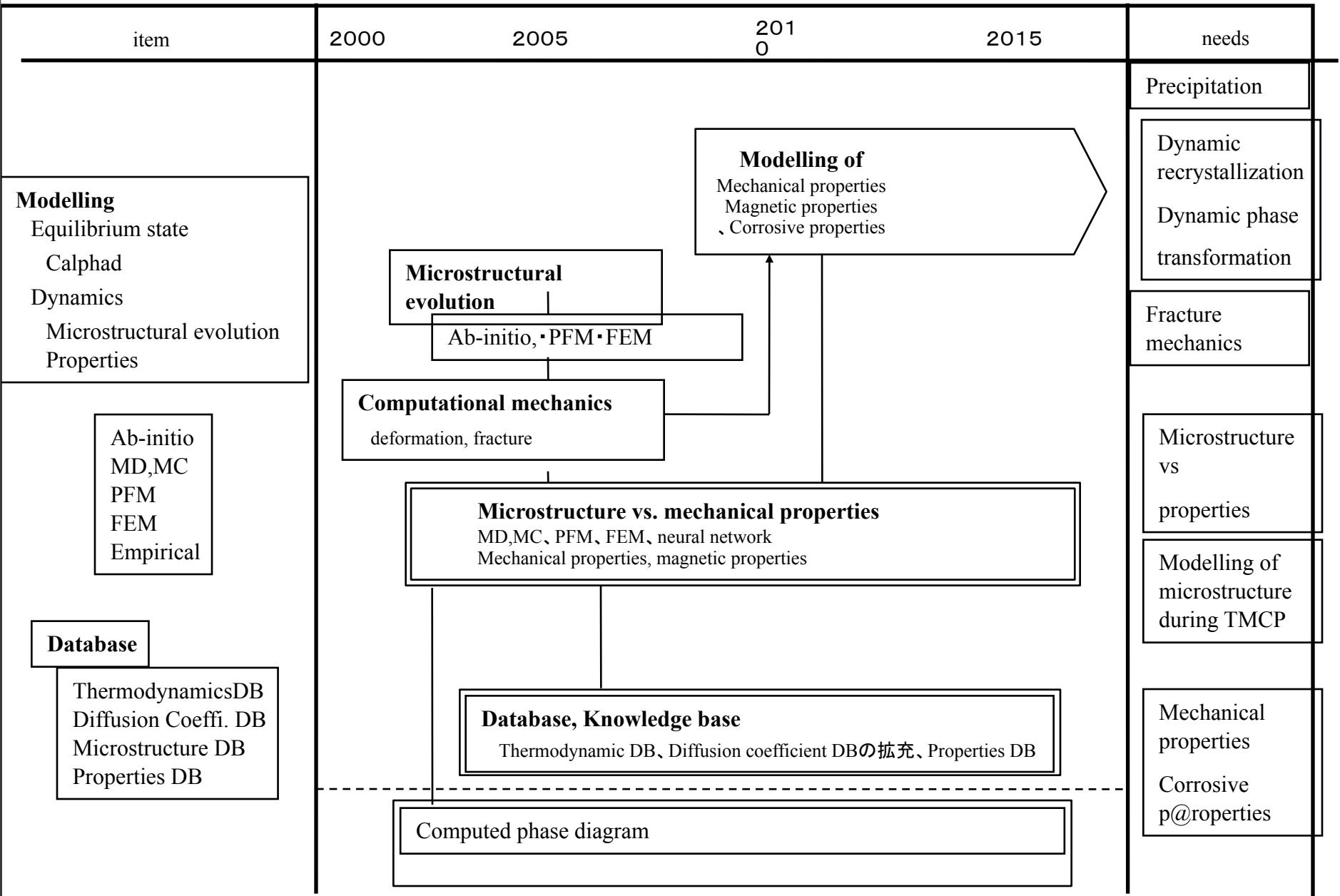


**Macroscopic  
analyses of giant  
straining process**

**Crystal plasticity  
analyses of  
dislocation  
accumulation**

**Phase field simulation of  
microstructural  
evolutions**





# Multiscale 3D-model

## Microstructure

Phase field+MC and FEM

## Properties

FEM

Neural network